OPTICAL NOISE PERFORMANCE IN SMF-REACH AND SMF-REDUCED SLOPE FOR RAMAN FIBRE AMPLIFICATION USING DIFFERENT PUMPING TECHNIQUES

BY

ISOE GEORGE MOSOTI

SC/PGP/006/11

A THESIS SUBMITTED IN PARTIAL FULFILLMENT OF THE REQUIREMENT FOR THE AWARD OF MASTER OF SCIENCE DEGREE IN PHYSICS, SCHOOL OF SCIENCE, UNIVERSITY OF ELDORET

2014

DECLARATION

DECLARATION BY THE STUDENT

This thesis is my own original work and has not been presented for a degree in any other University or institution. No part of this thesis may be reproduced without the prior written permission of the author and University of Eldoret.

Isoe George Mosoti

SC/PGP/006/11

Signature …….……. Date.……

APPROVAL BY THE SUPERVISORS

This thesis has been submitted for examination with our approval as University Supervisors.

Dr. Kennedy M. Muguro,

University of Eldoret,

Eldoret

Signature…….……. Date ……

Dr. David W. Waswa,

University of Eldoret,

Eldoret

Signature…….……. Date……

DEDICATION

This work is not only dedicated to all those who have inspired me, but also those we have shared the same dream.

ABSTRACT

Signal amplification in optical fibres during transmission has become one of the techniques in improving capacity and reach in telecommunication networks. Fibre Raman amplifiers (FRAs) are currently being adopted in many long-haul signal transmission systems and passive optical networks (PONs), for metropolitan applications due to their ability to offer longer amplification spans and wider bandwidth. The fact that signal amplification is distributed in FRAs is the major advantage of their application. In this case the signal is amplified along the fibre during propagation, a fact that drastically reduces the system nonlinearities. Although FRAs are basically low noise amplifier, they are still subjected to several noise sources which limit the amplifier performance. In this work, two pumping techniques namely co-pumping and counter pumping were used both in the theoretical and experimental analysis of noise in FRAs. A low signal power of -10 dBm was used while pump power was either fixed or varied depending on a particular analysis. Two types of fibres, Single Mode Reach Fibre (SMF-Reach) and Single Mode Fibre Reduced Slope (SMF-RS) each of length 25 km and 50 km were used. It was found that the longer the fibre length, the higher was the on- off gain irrespective of the pumping technique used. The Co- pumping configuration provided a higher Raman on-off gain than counter pumping scheme. An on-off gain of 5.7 dB and 4.5 dB was achieved experimentally for co- and counter pumping schemes, respectively, for the 25 km SMF-Reach fibre. For a similar length of SMF-RS fibre, an on-off gain of 4.8 dB and 3.9 dB was achieved for co- and counter pumping schemes, respectively, for the 25 km fibre. For a 50 km fibre, an on-off gain of 6.6 dB and 5.1 dB was obtained for the two pump configurations respectively using SMF-Reach fibre. For a similar length of SMF-RS fibre, an on-off gain of 5.3 dB and 4.3 dB was achieved for co- and counter pumping schemes, respectively. The Optical Signal to Noise Ratio (OSNR) also increased with an increase in on-off gain. An OSNR of 12.8 dB and 12.3 dB was achieved experimentally for co- and counter pumping schemes, respectively, for 25 km SMF-Reach. For 50 km fibre, an OSNR of 10.0 dB and 9.3 dB was recorded for the two pumping schemes respectively. OSNR was also observed to vary inversely with fibre length. The pump reflection power was noticed to vary inversely with gain and directly with fibre length irrespective of the pumping scheme applied. Co- pumping scheme had a better OSNR performance in both fibre types. Similarly, counter pumping scheme had a higher Noise Figure (NF) and pump reflection power. A NF of -2.2 dB and -1.9 dB was achieved experimentally for co- and counter pumping schemes, respectively, for the 25 km SMF-Reach fibre. For a 50 km fibre, a NF of -1.8 dB and -0.7 dB was obtained for the two pump configurations respectively using SMF-Reach fibre. NF was also observed to vary directly with fibre length. The noise analysis implies that SMF-Reach fibre is a suitable candidate in signal transmission due to its higher OSNR and better Raman amplification. The results also clearly indicate that, the co-pumping technique would highly be recommended due to its improved noise performance and would be preferred most in optical communication networks. The findings of this study are significant and give insight toward the optimization of fibre Raman amplifiers in long haul signal transmission.

TABLE OF CONTENTS

LIST OF FIGURES

LIST OF ABREVIATIONS AND SYMBOLS

ASE - Amplified Stimulated Emission

DFB laser - Distributed Feed Back Laser

DOP - Degree of polarization

DRA - Distributed type Raman amplifier

DRS - Double Rayleigh scattering

EDFA - Erbium-Doped Fibre Amplifier

FRA - Fibre Raman amplifier

MPI - Multipath Interference

NF - Noise Figure

OFRA - Optical fibre Raman amplifiers

OSA - Optical spectrum analyzer

OSNR - Optical Signal to Noise Ratio

PMD - Polarization mode dispersion

PONs - Passive optical networks

RBS - Rayleigh back scattering

RIN - Relative intensity noise

SMF - Single Mode Fibre

SOA - Semiconductor Optical amplifier

SOP - State of polarization

SRS - Stimulated Raman scattering

VPI - Virtual Photonics, Inc

WDM - Wavelength Division Multiplexing

k - Polarization constant

A_{eff} - Effective core area of the transmission fibre

L_{eff} - Effective fibre length

g_R - Raman gain coefficient

α_s - signal attenuation

α_p - pump attenuation

ω_s - signal angular frequency

ω_p - pump angular frequency

V_g - Group velocity

k_s - Propagation constant at the signal frequency

E_{pH} - Photon energy of the signal

B_0 - Optical band width

r - Rayleigh scattering

P_{in} - input signal power

P_{ASE} - Unpolarized ASE noise power

n_{sp} - Spontaneous-scattering parameter (population inversion parameter)

h - Planck's constant

ACKNOWLEDGEMENT

Firstly, am very much grateful to the almighty God for the gift of life, good health and strength he gave me during the entire research period at the University of Eldoret. My deep and sincere gratitude goes to my supervisors Dr. Kennedy Muguro and Dr. David Waswa for their tireless input, many encouragements, constructive guiding comments, discussion, criticism, and all the necessary contributions they made that did not only make this work come out successfully, but also generated new ideas and perceptions toward this work. My gratitude also goes to the Physics Department of the University of Eldoret for the opportunity they gave me to undertake this project using some of their available resources especially the free internet services.

I extend my appreciation to Prof. Andrew Leitch and Prof. Tim Gibbon of Nelson Mandela Metropolitan University (NMMU), South Africa, for the three months invitation to use their Fibre Optics Research centre for my experimental demonstrations. Thanks also go to Enoch K. Rotich and Dr. Romeo of NMMU for the support and willingly assisting me to familiarize with the optical fibre measurement equipments during the research visit period. Special thanks to Mrs. Alta Beer for coordinating and efficiently executing every administrative task in regard to the smooth stay of my entire visit.

I am also obliged to all members of University of Eldoret Laser and Fibre Optics Research Group for their company, encouragement and support throughout the research period. Finally, I extend my gratitude to all my family members, my dad and mum Mr. and Mrs. Isoe, my beloved sisters Annette and Emmy for their moral support and continuous encouragement they have accorded to me during this straining period, sincere

gratitude to my fiancée Metrine for being very supportive, understanding, and patient all along.

CHAPTER ONE

INTRODUCTION

1.1 Background

Fibre-optic communication is a method of transmitting information from one place to another by using light as a carrier. Light pulses bearing information are sent through an optical fibre which is normally deployed between the transmitter and the receiver [1]. An optical fibre is a dielectric medium commonly made of silica or plastic filament used in optical communication network for broadband communication to transmit information via light signals [2]. Materials such as plastic filament have been used to make fibres but these types of fibres are not used in optical communication networks. Optical fibres are able to guide light by using the principle of total internal reflection within the core/cladding interface [3].

1.2 Advantages of Optical Fibres

There are several advantages associated with optical fibre technology, which includes:

i) Broad band communication where video signal, microwave signal, and data from computers can be modulated over light carrier wave and demodulated by optical receiver at the other end.

ii) The optical fibre is electrically non-conductive hence; it does not act as antenna to pick up electromagnetic signals which may be present nearby. This means that the information propagating in the optical fibre cables is immune to electromagnetic interference e.g radio transmitters, power cables adjacent to the optical fibre cables or even electromagnetic pulse generated by nuclear devices. This makes

optical fibres more suitable in sensitive information security applications areas like in military systems.

iii) There are various optical bandwidth windows in the optical fibre cable at which the attenuation loss is found to be comparatively low and so transmitter and receiver devices are developed and used in these lower attenuation regions. Due to low attenuation of 0.2dB/Km in optical fibre cables, it is possible to achieve long distance communication effectively over information capacity rate of 1Tbit/s.

iv) By using an optical fibre, a high degree of data security is afforded since the optical signal is well confined within the waveguide (with any emanations being absorbed by an opaque jacketing around the fibre), thus makes fibre attractive in applications where information security is important, such as banking computer networks and military systems.

There are also some drawbacks associated with optical fibre. These include:

i) The cost of fabricating a fibre. Even though the raw material for making optical fibres, sand is abundant and cheap, optical fibres are still more expensive per meter than copper.

ii) Optical fibres are more fragile than electrical wires.

iii) The glass can be affected by various chemicals including hydrogen gas (a common problem in under water cables).

With the fibre-optic technology, information (data) is sent over long distances successfully. However, the effect of polarization and other optical effects, still present in modern fibres demand further investigation. This will improve the performance of the

fibre especially in long haul transmissions and passive optical networks PONs. Some of optical effects impact on signal transmission negatively while others like Raman amplification, which is based on stimulated Raman scattering (SRS) have useful applications in fibre communication systems [4,5].

1.3 Signal Amplification

Due to increasing demand and the need of high speed data transmission, the capacity of modern optical communication system has taken an upward trend. One of the techniques that have been adopted in improving capacity and reach in telecommunication networks involve signal amplification in optical fibre during transmission [6]. Different types of optical amplifiers that have been used include; Erbium-Doped Fibre Amplifier (EDFA), Semiconductor Optical amplifier (SOA) and Fibre Raman amplifier (FRA). Fibre Raman amplifier has been found to be outstanding for optical amplification, both in long haul signal transmission and passive optical networks (PONs) for metropolitan applications [7, 8]. In this case the amplifier wavelength also known as pump wavelength λ_p is always less than the signal wavelength λ_s.

There are two main types of optical fibre Raman amplifiers (OFRA) namely, discrete (lumped) and distributed Raman amplifier [9].When the fibre is being pumped in the actual transmission span that links two points which is longer than 30 km, then we have distributed amplification. Distributed Raman amplifier (DRA) utilizes transmission optical fibre as the active medium [10]. One of the main advantages of employing DRA is that it increases the lengths of spans between signal regeneration sites. The

amplification bandwidth of Raman amplifiers is defined by the pump wavelengths and therefore amplification can be provided over wider and different regions than may be possible with other optical amplifiers which rely on dopants and device design [11].

In Raman amplification, the signal can either be propagated in identical direction as the pump (co-pumped), from the opposite direction (counter-pumped) or from both directions (bidirectional pumping). These pumping schemes have different signal gain and the peaks of the gains occur at pump-signal detuning of approximately 13.2 THz.

If the amplifier is contained in a box at the transmitter or receiver end of the system it is called a discrete Raman amplifier [12]. A Discrete Raman amplifier scheme uses a shorter length (5 km) of fibre at the transmitter or receiver end to carry out the amplification.

The fact that signal amplification is distributed in Fibre Raman amplifiers (FRAs) is the major advantage of their application. In this case the signal is amplified along the fibre during propagation, a fact that drastically reduces the system nonlinearities [13].

Other reasons for using Raman amplifiers than Erbium-Doped Fibre Amplifier (EDFA) or even Semiconductor Optical amplifier (SOA) include;

i) Raman amplification can occur at any signal wavelength by proper choice of the pump wavelength while EDFA wavelengths are determined by the resonant levels of the erbium at around 1550 nm.
ii) Raman amplification is based on stimulated Raman scattering (SRS) which is a nonlinear phenomenon that occurs in any fibre while EDFA require a specially fabricated fibre.
iii) Raman amplifiers have a lower noise figure compared to EDFA and SOA.

Despite the many advantages associated with FRA other challenges have also emerged which includes:

i) The pump power decreases along the fibre length due to linear absorption and scattering.

ii) Amplification of spontaneous Raman photons occurs when the pump power is increased to offset attenuation losses. These spontaneous Raman photons are coupled into the guided mode all along the length of the fibre resulting to increase in optical noise.

1.4 Statement of the Problem

Since the signal power exponentially decreases with fibre length, a means of recovering the signal is required. Raman amplification using the transmission fibre as the gain medium is a promising technology for the optical long haul dense wavelength-division-multiplex (DWDM) communication system. With the increase in distance of data transmission, more losses are experienced as a result of optical noise accumulation within the transmission fibre. Optical noise is one of the fundamental loss mechanisms which occur in all fibres during signal transmission. This optical noise can propagate over long distances with the signal. It can also limit the maximum improvement in effective receiver sensitivity, as well as limiting the maximum transmission spans. It is therefore significant to investigate and fully understand the onset of optical noise especially in modern fibres which are currently used as gain medium. Research in optical noise has so far been done using the old fibre which is known to be limited by high level of impurities as well as remarkable signal dispersion. However modern fibres have been improved in quality and are of low polarization mode dispersion (PMD). As a result

there is need to investigate and characterize the noise performance in modern fibre when used as a gain medium during Raman amplification. Current understanding of noise performance is therefore necessary and a major step toward the improvement of the overall efficiency of modern optical communication system.

1.5 Objectives

The specific objectives of this work were;

i) To measure the on-off gain of Co-pumping and Counter pumping schemes using modern fibres.
ii) To analyze the OSNR of SMF-Reach fibre at different pumping configurations.
iii) To analyze the NF of SMF-Reach fibre while considering the two pumping schemes.
iv) To evaluate the pump reflection power performance of single mode reach fibre (SMF-Reach) and single mode reduced slope fibre (SMF-RS) at co- and counter pumping schemes.

1.6 Justification/ Significance

With current increase in demand for broadband access to a faster and more reliable internet, the optical fibre Raman amplifiers are therefore expected to increase both the transmission span of the optical signal and the data rate. This can only be attained through proper amplification of the signals so that the transmitted signal attains maximum power with very minimal losses at the receiver end.

Raman amplifiers are good in terms of higher amplifier gains, longer transmission spans, wide bandwidth band as well as low noise levels. This study is of great significant in the improvement of transmission spans in optical communication system and also transmission of data with higher bit rates per second. It is a great contribution to the Information and Communication Technology (ICT) sector. This work is viewed as a major step towards realizing Kenya vision 2030, which will at the end contribute immensely to the world's growing economies and alleviate poverty.

CHAPTER TWO

LITERATURE REVIEW

2.1 Introduction

Raman amplification is a nonlinear effect which was first observed in 1928 [14], but attracted limited interest until 1962 when the phenomenon of stimulated Raman scattering was first discovered [15] Raman amplification technique in optical fibres is currently being utilized in optical communication networks to overcome signal attenuation within the optical fibre. In this chapter, the basics of Raman scattering in optical fibres have been discussed. Some relevant system impairment parameters that influence Raman gain and performance of the amplifier in communication systems have also been highlighted.

2.2 Raman Scattering

Raman scattering of light is an occurrence that is due to an inelastic nonlinear behavior of a dielectric medium, such as an optical fibre when subjected to a high intensity optical beam. In this case the effect is known as spontaneous Raman scattering. In the quantum mechanical description (Fig 2.1), Raman scattering is most easily understood and involves photon-optical phonon interaction. In the Raman scattering process, optical photons are elastically scattered by quantized molecular vibrations called optical phonons [16, 17]. These photons loose or gain energy to the molecular lattice resulting in scattered light of lower or higher frequency. The lower frequencies ω_s of scattered light are the Stokes-shift (Fig 2.1a) and the higher frequencies ω_p are called anti –Stokes shift (Fig 2.1b). The anti-Stokes process is very weak in fibres and plays no role in Raman fibre

amplifiers. This is because the occurrence of the anti-Stokes shift requires a population inversion in the vibration states, a process which cannot be easily achieved [18].

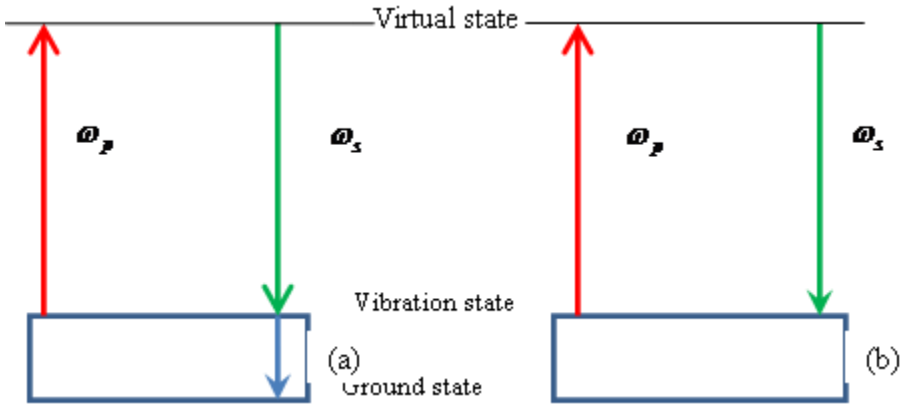

Fig 2-1: Scattering caused by energy transition of molecules from the ground state into excited state.

2.3 Stimulated Raman scattering (SRS)

Stimulated Raman scattering (SRS) is a nonlinear process which occurs when a light signal in the Stokes frequencies and a pump photon with high power are coherently coupled by the Raman process. This process results in the transfer of optical power from the pump to the signal and hence turns an optical fibre into a broadband amplifier. SRS was first observed in fibres by Stolen [19] and was initially considered a damaging nonlinear effect in Wavelength Division Multiplexing (WDM) systems where several channels (wavelengths) are coupled into the fibre simultaneously. This is because SRS can transfer power from a higher frequency channel to a lower one causing signal crosstalk [20]. The phenomenon of SRS process can be described quantum mechanically just like spontaneous Raman scattering. In this case, a pump photon is converted to a

second signal photon that is a replica of the first and the remaining energy is converted into an optical phonon. The virtual state (fig 2.2) is due to the fact that Raman scattering is non resonant and is therefore a very fast process [21].The continuum nature of molecular vibration state is due to the amorphous nature of silica i.e. silica has inconsistent physical and chemical properties. This distributes energy of a medium to different wavelengths [22].

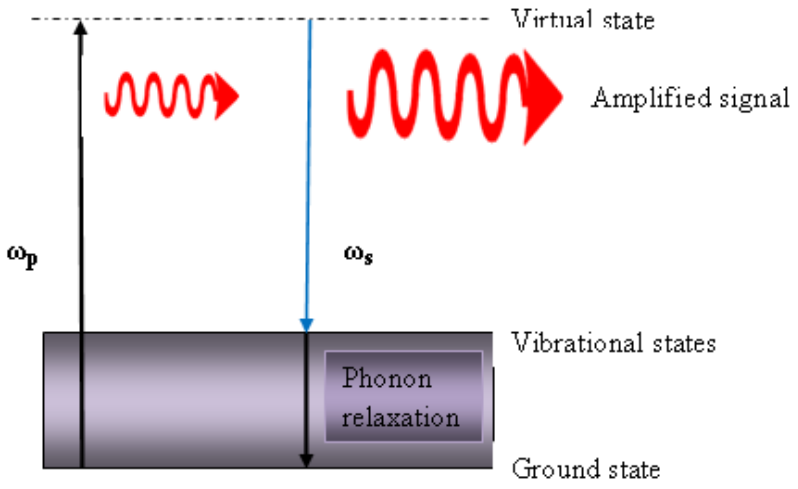

Fig 2-2: Quantum representation of Stimulated Raman scattering.

In cases of higher pump powers, the scattered light can grow rapidly with most of the pump energy being converted into scattered light hence giving rise to stimulated Raman scattering (SRS). At this high power levels, the nonlinear phenomenon of SRS leads to remarkable signal amplification in the transmission span. The intensity of the scattered light grows exponentially as the incident power exceeds a given threshold value. In the case of SRS, the thresh hold power P_{th} i.e. the minimum power levels at which the Raman process becomes stimulated and transfers most of the pump power to the stokes wave, is estimated as [23].

$$P_{th} = \frac{16A_{eff}}{kL_{eff}g_R} \quad \text{(2.1)}$$

where, k is the polarization constant, A_{eff} is the effective core area of the transmission fibre, L_{eff} is the effective fibre length and g_R is the Raman gain coefficient.

In the process of Raman amplification, the signal and pump power evolution over a given fibre length is governed by the following coupled equations;

$$\frac{dP_s}{dz} = g_R P_p P_s - \alpha_s P_s, \quad \text{(2.2)}$$

$$\mp \frac{dP_p}{dz} = -\frac{\omega_p}{\omega_s} g_R P_p P_s - \alpha_p P_p \quad \text{(2.3)}$$

where g_R ($W^{-1}M^{-1}$) is the Raman gain coefficient, α_s and α_p are the signal and pump attenuations coefficients respectively, while ω_s and ω_p is the signal and pump angular frequencies respectively. P_p and P_s are the pump and signal power respectively. The $\mp$ sign represents the backward and forward propagation of the pump wavelength respectively.

Equations 2.2 and 2.3 shows that the signal is amplified by the pump at a certain proportion, with the constant of proportionality being determined by the Raman gain efficiency, and losses as a result of attenuations in the optical fibre. If there is no pump power, i.e. in equation 2.3, g_R =0, then the pump power $P_p(z)$ as a function of distance (z) in a fibre of length L in the forward pumping scheme (P_f) is given as;

$$P_f = P_p(z) = P_0 e^{-\alpha p(l-z)} \text{.....} \quad (2.4)$$

While in the backward pumping scheme (P_b) is given as

$$P_b = P_p(z) = P_0 e^{-\alpha(z)} \text{.....} \quad (2.5)$$

Equations 2.4 and 2.5, shows that the pump power reduces as a result of energy transfer to the signal and attenuations along the transmission fibre. In order to overcome the problem of pump depletion, the pump must be set to operate at relatively higher powers compared with the signal power.

If the signal beam is pumped into the fibre from both ends (bidirectional pumping), the total pump power over a given fibre length is simply the sum of the pump powers in both directions given as:

$$P_B = P_f + P_b \text{.....} \quad (2.6)$$

where P_f and P_b can also be obtained by ignoring pump depletion.

$$\frac{dP_f}{dz} = -\alpha P_f \text{;.....} \quad (2.7a)$$

and

$$\frac{dP_b}{dz} = \alpha_p P_b \text{.....} \quad (2.7b)$$

Solving equations 2.7 (a) and 2.7 (b), the total pump power $P_p(z)$ over a fibre at a distance (z) is given in the form;

$$P_p(z) = P_0\left\{r_f \exp(-\alpha_p z) + (1-r_f)\exp\left[-\alpha P(l-z)\right]\right\}. \ldots\ldots\ldots\ldots\ldots\ldots\ldots\ldots\ldots\ldots (2.7)$$

where; $r_f = \dfrac{P_f}{P_b + P_f}$ and $0 \le r_f \le 1$ represents the fraction of forward pump power. If r_f =0 then the pumping becomes purely backward, if r_f =1, then it is a forward pumping scheme and if r_f =0.5, it implies a bidirectional pumping scheme with equal pump powers from both fibre ends.

2.4 Optical Noise and System Impairments

Designing a fibre Raman amplifier in most cases is a relatively simple task. However, managing the impairments that arise due to the nature of the optical fibre and the high optical power involved has been a far more discouraging task. In this section, the main impairments mechanisms strongly emphasized or specific to Raman-based systems are discussed. Double Rayleigh scattering (DRS) is one of the impairment discussed in this section. DRS is the mechanism responsible for Multipath Interference (MPI) noise, which can severely affect the transmission performance for a long-haul Raman based system.

With enough Raman gain in the span and little enough Amplified Stimulated Emission (ASE) noise, MPI presents the next important limit to long distance transmissions using Raman amplification.

2.3.1 Amplified Spontaneous Emission (ASE) Noise

Any amplified light signal suffers from optical noise which is normally generated in the amplification process. Amplified spontaneous emission (ASE) is an inherent noise which is present in all optical amplifiers. ASE noise is generated as a result of spontaneous

Raman scattering (SRS) during the process of optical amplification. Due to its random phases the ASE is generated in all directions in the fibre but in practice it exists only in the amplifier bandwidth. The ASE noise performance of a FRA can be best describe in terms of optical-signal-to-noise ratio (OSNR) which is defined as the ratio of the signal optical power to the power of the ASE with respect to a given reference bandwidth centered about the signal wavelength [24]. The OSNR is often referenced to 0.1 nm bandwidth when measured with the optical spectrum analyzer (OSA). This noise degrades the OSNR by adding a wider band of background noise around the signal wavelength hence affecting the general performance of any optical communication system [25]. The system OSNR can be improved by filtering the ASE at the amplifier output whereby an optical filter is placed just before the receiver. The OSNR at the amplifier output is defined as:

$$OSNR = \frac{g_R P_{in}}{P_{ASE}} = \frac{P_{in}}{2n_{sp}h\nu B_0} \quad \text{(2.9)}$$

where g_R is the Raman gain, P_{in} is the input signal power, P_{ASE} is the unpolarized ASE noise power, n_{sp} is the spontaneous-scattering parameter also known as population inversion parameter, h is Planck's constant, ν is the optical frequency of noise and B_0 is the optical bandwidth. The factor of 2 in equation (2.8) accounts for the two fibre polarization modes [26].

2.3.2 Multipath Interference (MPI) Noise

Multipath interference (MPI) is present in all optical transmission systems. Multiple signal paths are introduced into the transmission path through many different sources including discrete reflection sources e.g. connectors (components within the amplifier) and reflections caused by the distributed process of double Rayleigh scattering [27]. Transmission penalty is caused by the interference of a multiple (doubly) reflected (and hence delayed) signal interfering with the intended signal as shown in the figure 2.3.

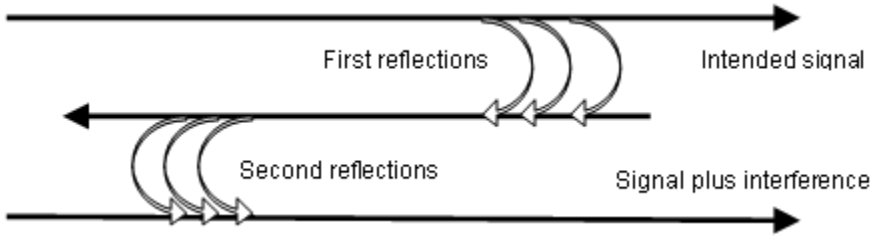

Fig 2-3: Double reflection causing interference with the intended signal.

In a Raman-amplified system, especially one with a chain of Raman amplifiers, MPI can easily result in performance limiting interference. The seriousness of the interference is due to the scattering light having passed two additional times through the Raman amplifier where it experiences the distributed gain [28]. The presence or absence of an optical isolator which is meant to eliminate the backward travelling signal in amplifier has a great impact on the analysis of MPI. In optical systems, with discrete amplifiers e.g. erbium doped fibre amplifiers (EDFA) the scattering sources can be separated from the amplifier by optical isolators. These isolators eliminate the backward travelling reflection and hence reduce the MPI by a great factor [29]. In distributed Raman-amplified systems the use of isolators to completely separate the sources of reflection and amplification is

not possible as both the amplification and the scattering sources are present in the transmission fibre [30].

2.3.3 Rayleigh Backscattering (RBS)

The phenomenon that limits the performance of a distributed Raman amplifier most in regard to optical noise generation is Rayleigh back scattering (RBS) [31]. RBS occurs in all fibre and is the fundamental loss mechanism for them. Although most of the scattered light escapes through the cladding, a part of backscattered light can couple into the core mode supported by single mode [32, 33]. However, it can be amplified over long lengths in fibres with distributed Raman gain.

RBS affects the performance of Raman amplifiers in two ways. Firstly, a part of backward- propagating Amplified stimulated emission (ASE) can appear in the forward direction, enhancing the overall noise. This noise is relatively small and is not of much concern for Raman amplifiers. Secondly, DRS of the signal create a cross-talk component in the forward direction that has nearly the same spectral range as the transmitted signal (in-band cross talk) [34, 35].

RBS in the transmission fibre must be taken into account when calculating the performance of high-gain Raman amplifiers. Backward travelling ASE will be reflected in the forward direction experiencing gain before reaching the receiver. This as well as spontaneous emission experiencing multiple reflections will degrade the Signal to Noise Ratio (SNR) thus degrading the performance of the amplifier [36]. Consequently, RBS limits the maximum improvement in effective receiver that can be obtained from implementing a Raman amplifier. The optical SNR at the receiver input of an optical

amplifier can be calculated from the following differential equations for the forward, p_s^+ and backward, p_s^- travelling power levels of the signal and spontaneous emission [37, 38].

$$\frac{dp_s^+(z)}{dz} = M_r p_p(z)(p_s^+(z) + E_{pH}B_0) + rp_s^-(z) - \alpha_s p_s^+(z), \quad \text{..... (2.12a)}$$

$$\frac{dp_s^-(z)}{dz} = -M_r p_p(z)(p_s^-(z) + E_{pH}B_0) - rp_s^+(z) + \alpha_s p_s^-(z). \quad \text{..... (2.12b)}$$

Where, E_{pH} is the photon energy of the signal, B_0 is the optical band width, r represents Rayleigh scattering.

$\pm M_r p_p(z)B_0$ Is the spontaneous Raman emission while $M_r p_p(z)$ is the rate in photon per length. All spontaneous emitted photons propagate along the fibre hence experiences amplification. The terms $+rp_s^-(z)$ and $-rp_s^+(z)$ represents Rayleigh back scattering. Pump depletion has been neglected because the signal and noise remains at low powers compared to the pump power at any given point with significant Raman gain.

2.3.4 Relative Intensity Noise (RIN)

Because stimulated Raman scattering is a non-resonant process, it is inherently fast, occurring over sub-pico-second time scales [39]. Therefore, pump power fluctuations can, in principle, be transferred to signals as noise. In fiber amplifiers, however, pumps and signals interact over time scales that are considerably longer because they propagate along many kilometers of fibre. This produces an averaging effect that limits the bandwidth over which pump noise is transferred to the signals [40]. This phenomenon

can be described in the frequency domain as a transfer of relative intensity noise (RIN) from a pump to a signal.

The co- and counter pumped cases are different because of the amount of averaging that occurs when a given slice of the signal light propagates along the fiber, overlapping with different slices of pump light. In the case of counter pumping, the signal and pump pass through each other, and averaging greatly reduces the impact of pump fluctuations above a few kilohertz [41]. As a rough estimate, significant reductions in RIN transfer occur for any pump fluctuations with a period larger than the propagation time through an effective length. For co-pumping however, the pump and signal only pass through each other if there is walk-off caused by chromatic dispersion. Therefore, averaging only reduces RIN transfer at much higher frequencies [42].

2.4 Optical Signal to Noise Ratio (OSNR) due to Double Rayleigh Scattering (DRS)

The use of optical isolators and reasonable specification for some components reduces most sources of MPI (reflections) in practical Raman amplifier systems except that caused by DRS. Rayleigh scattering is caused by small-scale in-homogeneities (compared to the wavelength of light) of the refractive index of the transmission fibre [43].

Fibre loss due to Rayleigh scattering reflections is characterized by a loss coefficient α_r such that for power travelling in the forward direction, $p^+(z)$ the following holds;

$$\frac{dP_s^+(Z)}{dZ} = -\alpha_r P_s^+(Z). \quad \text{(2.13)}$$

Rayleigh scattering occurs in all directions [43] the backward travelling signal $p^{-}(z)$ is given by;

$$\frac{dP_r^{-}(Z)}{dZ} = -r_s P_s^{+}(Z). \quad \text{.....} \quad (2.14)$$

Our main concern is the power that is doubly reflected. For the case of an unsaturated amplifier, (i.e. there is no pump depletion) the equation for the signal to –DRS noise ratio can be derived [44, 45].

DRS can be investigated by analyzing the power evolution of three signals: $p_s^{+}(z)$ is the forward travelling signal, $p_r^{-}(z)$ is the backward travelling signal-reflected light, and $p_r^{+}(z)$ is the forward travelling double-reflected light [46].

Assuming that the DRS energy is much smaller than the signal power, and neglecting additional reflections, the propagation of the three signals can be described by the following equations [43];

$$\frac{dP_s^{+}(z)}{dz} = \vec{g}(z)P_s^{+}(z), \quad \text{.....} \quad (2.15a)$$

$$-\frac{dP_r^{-}(z)}{dz} = \bar{g}(z)P_r^{-}(z) + r_s P_s^{+}(z), \quad \text{.....} \quad (2.15b)$$

$$\frac{dP_r^{+}(z)}{dz} = \vec{g}(z)P_r^{+}(z) + r_s P_r^{-}(z). \quad \text{.....} \quad (2.15c)$$

Equations 2.15a, 2.15b and 2.15c, represents the forward propagation signal, the backward propagation of the signal after a signal reflection and the forward propagation of the signal after two reflections.

The forward and reverse gain per unit length of the fibre is $\vec{g}(z)$ and $\bar{g}(z)$, are both given as;

$$\bar{g}(z) = \vec{g}(z) = g_R P_p(z) - \alpha_s . \quad (2.16)$$

To help solve these linear, first-order differential equations, the following integrating factors that physically represent the gain for forward traveling signal from z_1 to z_2 $\vec{G}(z_1, z_2)$ and the gain for a reverse traveling signal from z_2 to z_1 $\overleftarrow{G}(z_2, z_1)$ are introduced, hence we have;

$$\vec{G}(z_1 z_2) = e^{\int_{z_1}^{z_2} \bar{g}(\xi) d\xi} . \quad (2.17)$$

$$\overleftarrow{G}(z_1 z_2) = e^{-\int_{z_2}^{z_1} \bar{g}(\xi) d\xi} . \quad (2.18)$$

Applying boundary conditions, $P_r^-(l) = 0$ and $P_r^+(0) = 0$ we can solve for $P_r^+(l)$ and $P_s^+(l)$;

$$f_{DRS} = \frac{P_r^+(l)}{P_s^+(l)} = r_s^2 \int_0^l dz_2 \int_0^{z_2} \vec{G}(z_1, z_2) \overleftarrow{G}(z_2, z_1) dz_1 . \quad (2.19)$$

In general, this equation can be solved numerically by considering an ideal distributed amplifier with gain as unity i.e. ($G(z) = 1$) at all positions along the fibre [47] to have;

$$f_{DRS} = \frac{1}{2} r_s^2 l^2 . \quad (2.20)$$

Equation 2.20 demonstrates that DRS increases as the square of the fibre length. It also grows as the square of linear gain of the amplifier. This is only true for an ideal distributed amplifier [48].

2.5 Polarization Properties of Double Rayleigh Scattering (DRS)

In long fibre with low birefringence, Rayleigh scattering preserves the state of polarization and reduces the degree of polarization (DOP) to one third its original value [49] After DRS, the DOP has been calculated to be reduced by one ninth [50]. Assuming that the DOP of the DRS power was reduced to zero, the DRS light could then be considered to be unpolarized. In such a case, the amount of DRS light that will contribute to degrading the signal would be one half. However, since the DOP is actually one ninth, half of the remaining eight ninth is available to interfere with the signal in addition to the one ninth that is polarized. As expected, this depolarization has an effect on the impact of DRS. Therefore; the correction factor for the DRS noise is five ninths [51].

$$OSNR_{MPI}^{P} = \frac{5}{9} OSNR_{MPI} \quad \text{(2.21)}$$

This correction is critical as only MPI that is in the same polarization as the signal produces beat noise in the receiver.

2.6 Noise Figure (NF)

Basically, the noise figure (NF) is the ratio of the signal to noise ratio (SNR) at the input of an amplifier to that at the output of an amplifier i.e.

$$NF = \frac{SNR_{input}}{SNR_{output}} \quad \text{(2.22)}$$

Where, SNR is defined as the ratio of signal power to noise power i.e.

$$SNR = \frac{Signal\_power}{Noise\_power} \quad \text{(2.23)}$$

In situations where two amplifiers are cascading to each other and the gain of the first amplifier is lower than that of the second one, then the NF of the system is given as:

$$NF = NF_1 + \frac{NF_2 - 1}{G_1} \quad \text{(2.24)}$$

Where, G_1 is the gain of the first amplifier, NF_1 and NF_2 is the noise figure of the first and second amplifier, respectively.

NF can also be defined in terms of ASE noise. In such a case, NF can be approximated by taking measurements of the noise power added by the amplifier (p_{ASE})

$$NF = \frac{1}{G}\left(1 + \frac{p_{ASE}}{E_{pH} B_0}\right) \quad \text{(2.25)}$$

where, G is the on-off gain, E_{pH} is the photon energy of the signal, B_0 is the optical band width and p_{ASE} is the noise power [52].

2.7 Optical Noise Analysis

Other than the numerous achievements made so far in improving the state-of-the-art of optical systems, many issues concerning the future of the system in terms of efficiency and the increasing demand for capacity and reach still need to be adequately addressed. In particular, the effect of nonlinear interaction in optical fibres especially at higher optical powers is still a subject of great concern. More attention is required especially on modern fibres which are currently being adopted in many long-haul systems. Modern

fibres have low attenuation of ≤0.2 dB/km, but this value is still large enough to limit the transmission distances to a few hundred kilometers due to problems related to attenuation. This problem of attenuation was initially approached using optoelectronics repeaters in long-haul systems [53].

However, optoelectronics repeaters were prone to signal regeneration which was their major drawback because of the numerous repeaters required in the system which lowered the speed of electronics. Optical amplifiers development in the early 90‟s brought a new revolution in the fibre communication. They resulted in the elimination of repeater systems and a new down to all-optical systems with increased capacity. Optical amplifiers are associated with great amplification bandwidth which has enhanced the application of dense wavelength division multiplexed (DWDM) transmission. DWDM technique owes its success to the introduction of optical amplifiers and has resulted in increased capacity and span.

Optical time division multiplexing (OTDM) was also another technique that had been proposed as an alternative method for increasing the fibre transmission capacity [54]. This technique was widely applied on Erbium-doped fibre amplifier (EDFA) due to its high performance and stable dynamic behavior. As a result EDFA has been highly exploited close to its theoretical limits such that its lowest noise figure (NF) is close to the quantum limit of 3 dB. This NF is still a major limitation to state of the art systems. The high power associated with the EDFA amplified WDM system is a source of nonlinear signal impairments which are known to affect the performance of optical devices such as compensators [55]. These nonlinearities are caused by induced nonlinear

refractive index which occurs when a fibre is subjected to a high intensity beam [56]. Unlike the old fibre technology, modern fibre technology has ensured low water attenuation peak around 1400 nm in conventional Single Mode Fibres (SMF) [57]. This means that there is more usable bandwidth in such fibres for better transmissions.

A lot of research on Raman amplification has been carried out in optical fibre since 1970‟s [58]. due to its great potential in increasing usable bandwidth and the availability of higher power lasers. The full potentials of Fibre Raman amplifier (RFA) in optical communications and other new applications are yet to be totally exploited. Most of the results have been obtained using the old fibre which is limited to higher signal dispersion, higher PMD, fibre defects and undesired impurities. As a result, several modern fibres have been developed and are of low PMD and low dispersion. This work has picked on two modern fibres, SMF-Reach and SMF-RS and their on-off gain, OSNR, NF and pump reflection power investigated at both co-and counter pumping techniques. The relation between on-off gain, OSNR, NF and pump reflection power still needs to be analyzed especially when these modern fibres are used in optical networks. This approach is unique in the sense that it deviates from earlier analyses where no attempt was made to compare various parameters when fibres are used in optical networks. Optical noise effects in optical fibre are also very significant in regard to the operation and stability of modern optical communication systems as well as optical devices.

CHAPTER THREE

METHODOLOGY

3.1 Research Design

The approach to this study involved simulations as well as experimental analysis. Virtual Photonics, Inc. (VPI), version 9.0 software was selected to be used in the simulation approach [59]. VPI is a comprehensive simulation package developed by VPIphotonics GmbH. It is the latest and among the best photonics software, currently used by researchers and engineers in their photonics modeling innovations. This software enable users to plan, test, and simulate optical links in the transmission layer of modern optical networks.

3.2 Simulation Setup

Fig 3.1 shows the simulation set up of a distributed fibre Raman amplifier.

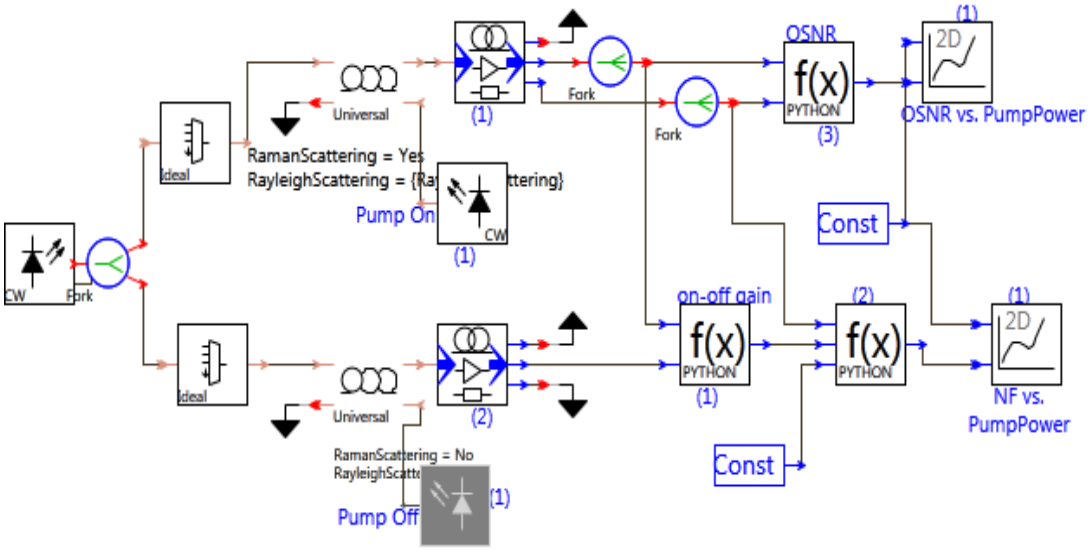

Fig 3-1: Set up of a distributed FRA at different pumping schemes using Virtual Photonics, Inc. (VPI) version 9.0

A CW Laser source was modeled to produce a continuous wave (CW) optical signal. This module (CW Laser source) was set to produce photons of a CW laser with a power of - 10 dBm at 1550 nm frequency throughout the experiment. The signal power was then directed into the fork module. The fork module copied particulars from its input to each of its output. This module was generally used to connect a single output port, to multiple input ports. The signal source from each of the fork output was then coupled with the pump using the WDM coupler. The pump Laser CW module was also modeled to produce a continuous wave (CW) optical signal. This module was set to produce photons of a CW laser with a power of up to 25 dBm at 1450 nm frequency throughout the experiment. This was meant to ensure maximum amplification of the signal which in RFA occurs when the pump-signal detuning is 100 nm. Both (signal and pump) were then propagated in a 25 km and 50 km Universal Fibre model, which was set to simulate a wideband nonlinear signal transmission in optical fibres with piecewise constant parameters specified for each fibre span individually, taking into account bidirectional signal flow, stimulated and spontaneous Raman and multiple Rayleigh scattering at each joint between spans. The output of the fibre was then connected to an optical signal/noise power meter module. This module had a central frequency bandwidth which was set at 1550 nm thus enabling the signal frequency to be sampled out from the noise frequencies, and directed to the signal output. Each input optical band was checked for whether it fell into the spectral range defined by parameters CenterFrequency and Bandwidth. If it did, whether to some extent or completely, the band would be kept. Those bands outside the window were directed into the noise output.

The signal power outputs (with pump on and with pump off) from the two signal/noise power meters (1 and 2) were then directed onto the Mathematical Expression (Python) module (1) where the on-off gain was calculated by simply taking the difference of the two. This module implemented the calculation of mathematical functions of one, two, three or four variables. The module uses the co-simulation interface and calls the Python interpreter to evaluate the expression. The on –off gain from the output and the noise power from signal/noise power meter (1) was then directed into Mathematical Expression (Python) module (2) where the NF was calculated and its results directed to the NumericalAnalyzer2D module (1). The OSNR was also calculated using Mathematical Expression (Python) module (3) and its results directed to NumericalAnalyzer2D module (2).

The NumericalAnalyzer2D module worked as an interface to the VPIphotonicsAnalyzer tool for two-dimensional numerical data. The NumericalAnalyzer2D module is a dual-input analyzer for numerical data. The module can display data as an X/Y plot and as a numeric worksheet. The X plot values like pump power, fibre lengths were swept using the Const. module.

3.3 Experimental Setup

Fig. 3.2 shows the experimental setup of a fibre Raman amplifier used in the experimental work done at the optical fibre research unit laboratory at Nelson Mandela Metropolitan University- Port Elizabeth, South Africa, during a three months research visit.

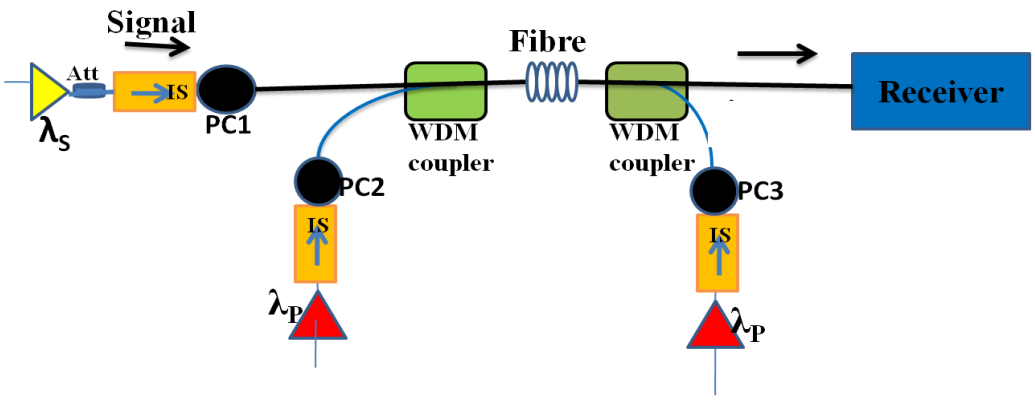

Fig 3-2: Experimental setup of a distributed FRA at different pumping schemes.

Two Raman pumps operating at frequencies of 1450 nm (λ_p) with a maximum output power of 25 dBm and a tunable laser source (λ_S) operating at a C band were used. The variable optical attenuator was connected to the signal to vary the amount of power getting to the receiver so as to attain the optimum signal power required. An isolator was connected to the pump and signal laser sources to maintain the signal in one direction thus protecting the laser sources from the counter-propagating laser light. The states of polarization (SOPs) of the signal and the pump were controlled using polarization controllers (PCs). Consequently, both the signal and pump were coupled on to the same fibre.WDM filters were used to combine and separate the signal and the pump onto and out of the fibre, respectively. Two fibre types; SMF-Reach and SMF-Reduced Slope (RS), each of length 25 km were used. The output was monitored using a power meter and an optical spectrum analyzer (OSA).

CHAPTER FOUR

RESULTS AND DISCUSSION

4.1 Overview of the Results

In this chapter, experimental and theoretical results that were obtained in the analyses of noise performance of a Raman amplified optical communication system are presented. The characterization of the laser pumps diode sources is first reported. This was essential because it was important to find the optimum working condition of the laser sources used. This is then followed by the signal gain and pump reflection where comparison of SMF-Reach and SMF-RS fibres is done. This is then followed by the results of On-off gain; OSNR and NF analysis of SMF-Reach fibre.

4.2 Characterization of the Laser Sources

Fig 4.1(a) shows the output characteristic of the pump that was used in the measurement.

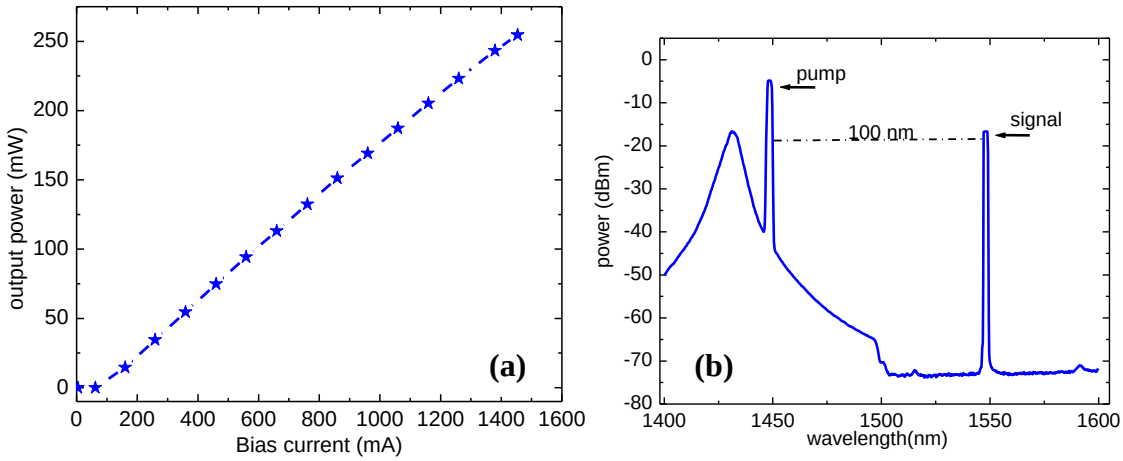

Fig 4-1: Output power as a function of input bias current, (b) wavelengths of the pump and signal at the fibre output.

Single mode GVT 074 laser diode operating at a high power range with a lasing threshold of about 62 mA of bias current and maximum power of 254.6 mW at 1454.3 mA was

used as shown in Fig 4.1 (a). Beyond the lasing threshold the pump output power increased linearly with the bias current.

The pump and signal wavelengths as recorded at the fibre output using an optical spectrum analyzer (OSA) is shown in Fig 4.1(b). The pump and signal wavelengths were coupled into a SMF fibre using a WDM coupler and then their signatures were obtained using an OSA at the fibre output. From the results in Fig 4.1 (b), the peak of the signal is at 1548 nm which is exactly 100 nm detuning from the pump wavelength which is the required detuning for Stimulated Raman Scattering (SRS) to occur in a fibre.

4.3 Raman gain profile for SMF-Reach fibre

Fig 4.2 shows the experimental and simulation results of Raman gain profile over a frequency range between 1530 nm and 1570nm. These results were obtained, using a 25 km SMF-reach fibre in the co-pumping configuration.

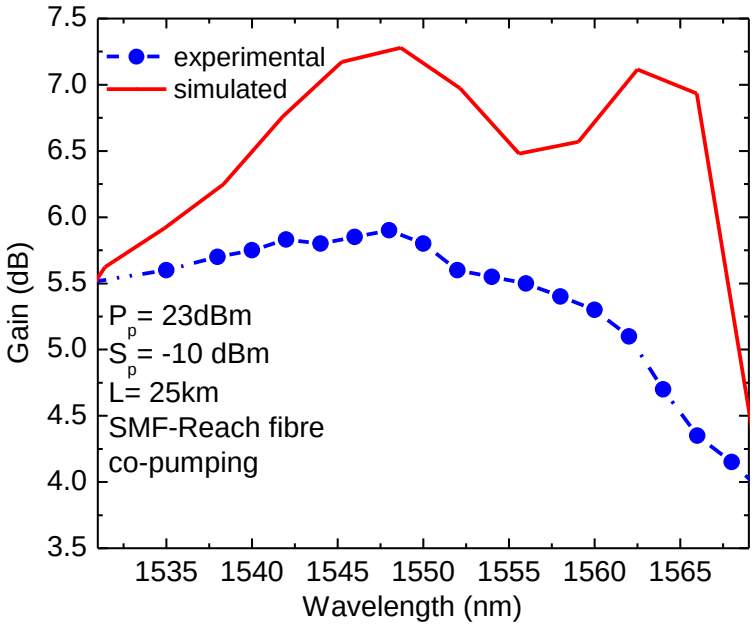

Fig 4-2: Raman on-off gain as a function of signal frequency for both experimental and simulation results.

Both simulation and experimental results in Fig 4.2 showed the existence of frequency shift which is attributed to the non-crystalline nature of silica glass. That is, the fibre has inconsistent physical and chemical structure, which allows molecular vibration frequencies produced as a result of SRS to spread out into overlapping band and creates a continuum [60].

The power from the pump was also distributed to all the signal frequencies within the bandwidth to supply gain but with different magnitudes. A maximum gain of 5.8 dB was attained experimental at 1548 nm which was exactly 100 nm detuning between the pump and signal wavelength thus the best detuning for SRS.

However in the simulations, a higher gain of 7.2 dB was attained under the same pump and signal wavelength and power. This is because simulations assumed that passive components like connectors, isolators and WDM filters maintained the same SOP through the transmission span. This component adds up losses to the signal during experimental measurements. This accounts for the higher gain recorded in the simulation compared to the one measured experimentally.

4.4 On-Off Gain Comparison of SMF-Reach and SMF-RS Fibres

Fig 4.3(a) and (b) show the experimental results of on-off gain variation with pump power for co- and counter pumping schemes at 25 km and 50 km fibre lengths. From Fig 4.3 (a) and (b), co-pumping recorded a higher gain of 5.7 dB and 4.8 dB for SMF-Reach and SMF-RS at 25 km respectively. When the fibre length was increased to 50 km, a much higher gain of 6.6 dB and 5.3 dB was attained for the SMF-Reach and SMF-RS fibre types respectively at 23 dBm pump power. On the other hand, counter pumping

recorded a gain of 4.5 dB and 3.9 dB over the same fibre types and pump power, at 25km fibre length. When the fibre length was increased to 50 km, a slightly higher gain of 5.1 dB and 4.3 dB was also recorded for the same fibre types.

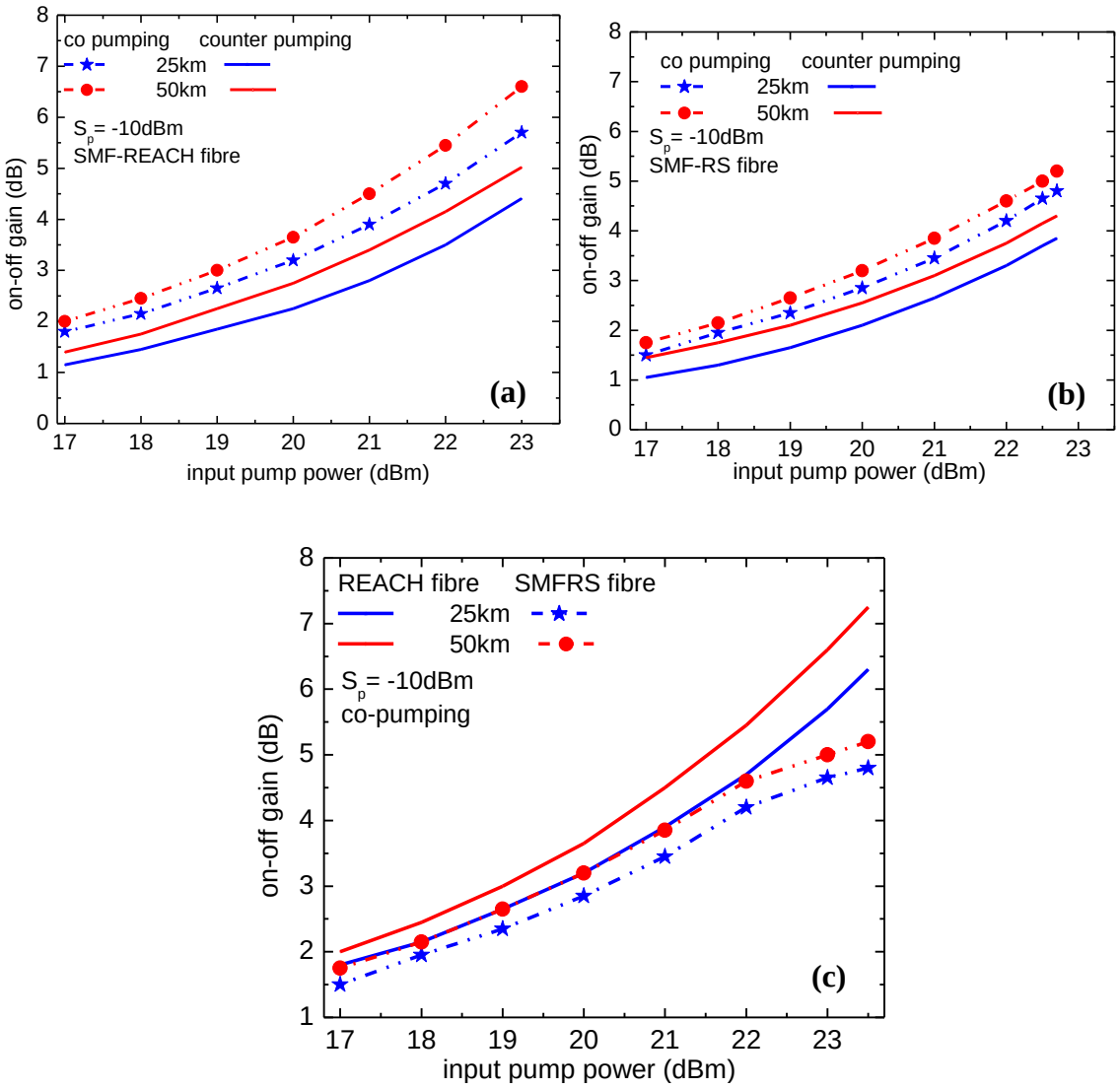

Fig 4-3: Experimental results of on-off gain variation with pump power (a) SMF-Reach fibre, (b) SMF-RS fibre, (c) on-off gain comparison for SMF-reach and SMF-RS fibres at co- pumping.

Results in Fig 4.3 imply that co-pumping produced a better performance in terms of gain in both fibres. This is because for the case of co-pumping, both the pump power and the

signal power were propagated in the same direction. This ensured that the pump was well utilized by the signal thus more pump power was transferred to the signal hence higher amplification levels were achieved. Also the ratio between the pump power and the signal power was maintained almost at the same level throughout the transmission span. In the case of counter pumping, the signal is propagated in a direction counter to the pump direction. This limit the pump to signal power transfer thus leaving much of the pump power unutilized hence accounting for the lower gain attained in this pumping scheme.

Fig 4.3 (c), gives the on-off gain comparison for SMF-reach and SMF-RS fibres at co-pumping. From Fig 4.3 (c), the SMF-Reach fibre gave a better performance in terms of gain than SMF-RS fibre due to the following fabrication improvements [61];

i. Ultra-low and stable polarization mode dispersion (PMD) to support the highest data rates with lower electronics costs.
ii. Low dispersion slope to provide denser wavelength division multiplexers (DWDM) channels and lower residual dispersion as well as less temperature variation.
iii. Optimized for both EDFA and Raman amplification to maximize system design options.
iv. Its high Raman efficiency enables more effective coupling of the Raman pump power into the optical signal – substantially better than fibers with a larger effective area.

4.5 Effects of pump power on pump reflection for SMF-Reach fibres during co- and counter pump configurations.

Fig 4.4 shows experimental and simulation measurements of the effect of pump power on pump reflection for co- and counter pumping scheme for 25 km SMF-Reach fibre.

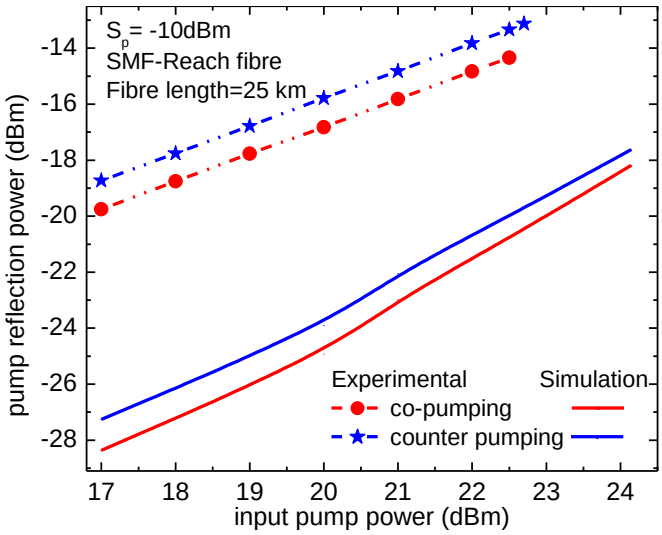

Fig 4-4: Experimental and simulation effects of pump power on pump reflection for a 25 km SMF-Reach fibre at co- and counter pumping scheme.

From Fig 4.4, the amount of pump reflection power was dictated by the pumping scheme used. This was attributed by the fact that in co-pumping, the signal power and the pump power both travelled in the same direction. This in turn ensured that there was more pump penetration into the signal thus more pump energy was transferred to the signal, leading to higher gains due to proper utilization of the pump. Very minimal pump power was therefore left unutilized in this pumping scheme thus the pump reflection power was very minimal.

For the case of counter pumping, the signal and the pump both propagated in a direction opposite to each other. This meant that there was minimal pump to signal power transfer thus much of the pump power was left highly unutilized. This unutilized pump power

was then reflected back and detected as pump reflection power thus accounting for the higher pump reflection power recorded in the counter pumping scheme.

4.6 Effects of pump power on pump reflection for SMF-Reach fibres at different fibre lengths.

Fig 4.5 (a) shows experimental and simulation results of the effect of pump power on pump reflection for 25 km and 50 km SMF-Reach fibre lengths for the co-pumping scheme.

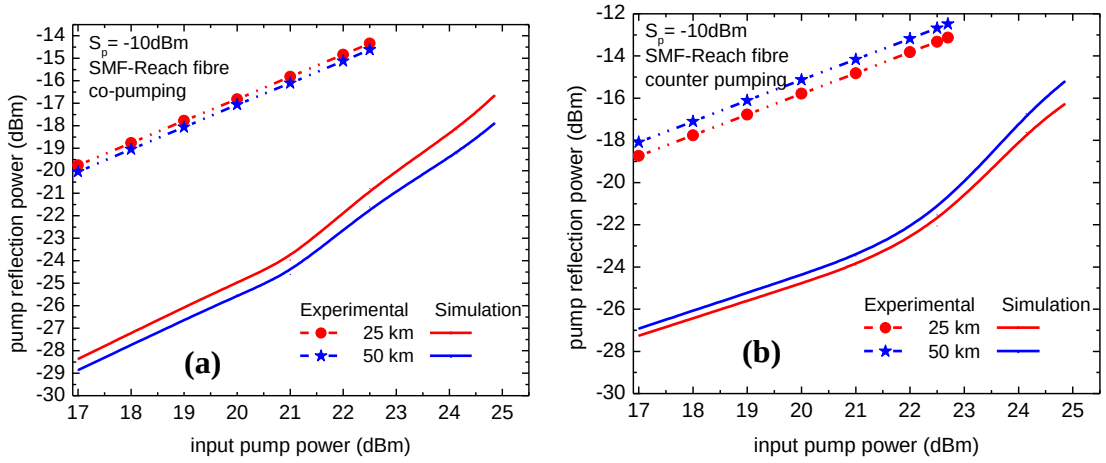

Fig 4-5: Experimental and simulation effects of pump power on pump reflection for (a) 25 km and 50 km SMF-Reach fibre at co- pumping, (b) 25 km and 50 km SMF-Reach fibre at counter pumping.

It can be seen that an increase in fibre length lead to a decrease in pump reflection power in the case of co-pumping scheme. This was attributed by the fact that as the fibre length was increased, the contact time between the pump and the signal also increased, thus more of the pump power was utilized and less was reflected back.

In the case of counter pumping, an increase in fibre length lead to a further increase in pump reflection power as shown in Fig 4.5(b). This is because as the fibre length is increased, the pump and the signal had to cover a longer distance hence weakening

further due to attenuations within the fibre. The ratio between the pump and the signal also reduced significantly as the pump approached a stronger signal from the opposite end of the fibre. This in turn limits the pump to signal power transfer by a greater factor. The unutilized pump power is then reflected back and detected as pump reflection power.

Simulation results in Fig 4.5 (a) and (b) gave a lower pump reflection compared to the experimental results in both pumping schemes because the passive components used in the experimental work reflected much of the power, which was not the case in simulation.

4.7 On-Off Gain Analysis of SMF-Reach Fibre Using a DFB Power Source

Fig 4.6 illustrates how on-off gain varies exponentially with pump power. In the experimental measurements, for pump powers less than 17 dBm, a lower on-off gain of 1.7 dB and 1.8 dB was recorded for a 25 km and 50 km fibres respectively.

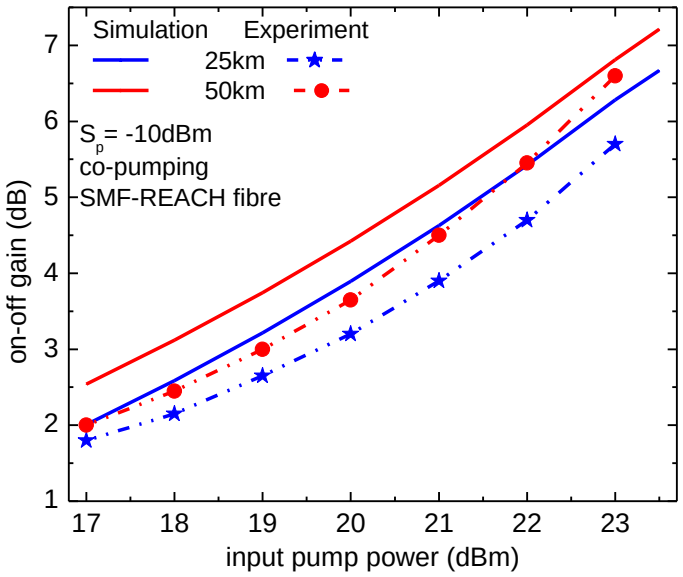

Fig 4-6: Experimental and simulation comparisons for on-off gain evolution with pump power for co-pumping.

This is because the pump power over this region was not powerful enough to induce remarkable SRS and thus minimal power was transferred from the pump to the signal

hence accounting for the small gain. With constant increase in pump power, the on–off gain increased exponentially up to a maximum of 5.7 dB and 6.6 dB for the two fibre lengths, respectively. The increase in pump power induced remarkable SRS which in turn enabled pump to signal power transfer, hence compensating for the attenuations within the fibre.

In the simulations, insertion losses from passive components like connectors, isolators and WDM couplers were not considered. These components added up losses to the signal during experimental measurements. This accounts for the higher gain recorded in the theoretical simulation compared to the one measured experimentally.

4.8 OSNR analysis in SMF-Reach Fibre at different pumping configuration

From the experimental results in Fig 4.7, the OSNR reduces gradually for co – pumping for pump powers ≥17 dBm because the pump power over this region was very weak to introduce SRS thus more noise was transferred from the pump to the signal thus a continuous reduction in OSNR.

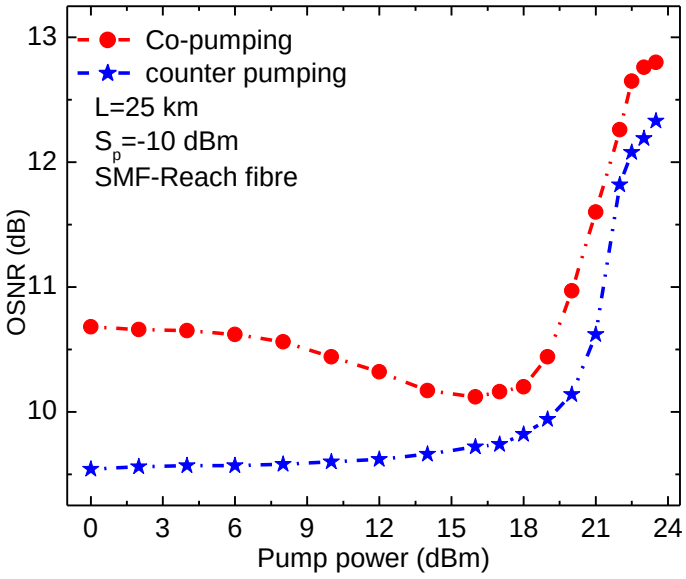

Fig 4-7: Experimental measurement of OSNR variation with pump power for co-pumping and counter pumping schemes.

The RIN noise contribution from the pump was dominant over this low power region. Counter pumping was more superior to RIN noise performance compared to co-pumping [62]. This accounts for the continuous drop in OSNR for co-pumping while the OSNR for counter pumping increases slightly over this low power range. However, as the pump power was increased beyond 19 dBm, the OSNR of both the pumping schemes also increased because the pump power over this region was now strong enough to amplify the signal thus accounting for the continuous increase in the OSNR. Co-pumping gave a better OSNR performance than counter pumping because for the case of co-pumping, both the pump power and the signal power were propagated in the same direction. This ensured that the pump was well utilized by the signal thus more pump power was transferred to the signal hence higher amplification levels were achieved. Also the ratio between the pump power and the signal power was maintained almost at the same level throughout the transmission span. For the case of counter pumping, the signal was propagated in a direction counter to the pump. This limited the pump to signal power

transfer thus leaving much of the pump power unutilized hence accounting for the lower OSNR attained in this pumping scheme.

4.9 OSNR Analysis of co-pumping scheme for 25 km and 50 km SMF-Reach Fibres

From experimental results in Fig 4.8, at pump powers beyond 17 dBm, a continuous increase in pump power resulted to a continuous increase in OSNR in both fibres because as the pump power increased, the pump became more powerful to compensate for losses within the transmission fibre.

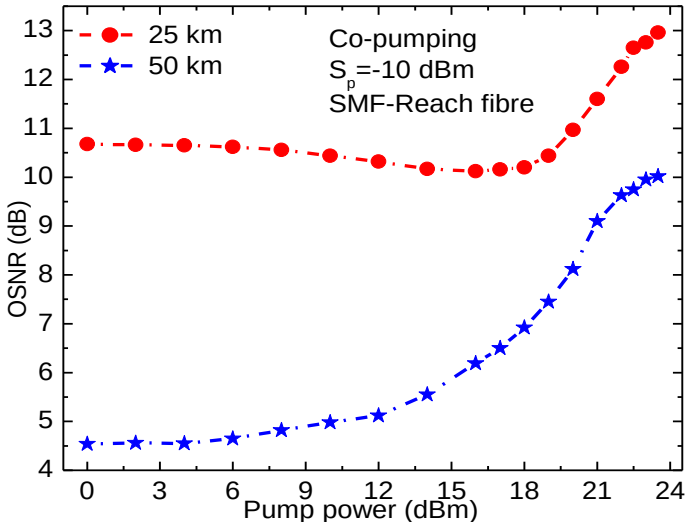

Fig 4-8: Experimental results of OSNR as a function of pump power at different fibre lengths for co-pumping scheme, (a), (b) Simulation.

A 25 km fibre recorded a higher OSNR of 12.8 dB compare to 10.3 dB recorded by a 50 km fibre at 23 dBm pump power because an increase in fibre length also lead to an increase in ASE noise accumulation within the fibre thus accounting for the drop in OSNR at longer fibre lengths.

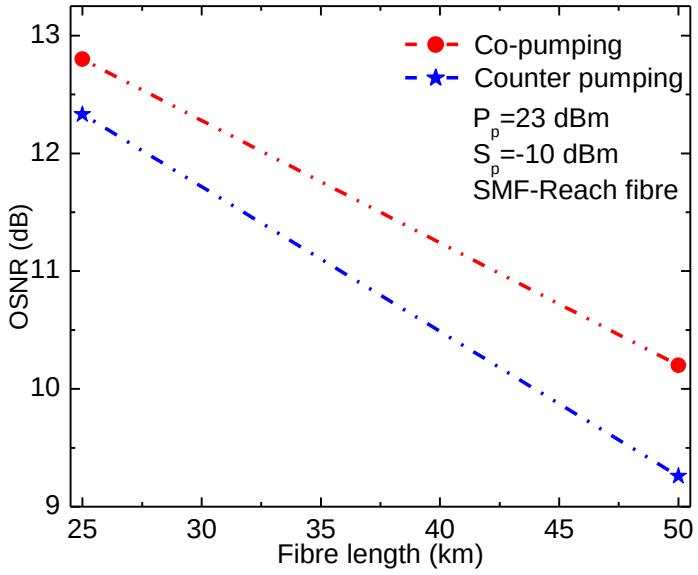

Fig 4-9: OSNR (dB) verses fibre length (km) at co- and counter pumping schemes.

Results in Fig 4.9 show the experimental measurements of the OSNR variations as a function of fibre length at different pump configuration. From Fig 4.9, the OSNR of both co- and counter pumping schemes reduced with an increase in fibre length. This was due to the losses within the fibre which increased with an increase in fibre length. As the fibre length was increased, the OSNR for counter pumping reduced greatly compared to that of co- pumping because for the case of counter pumping, the pump power was not well utilized by the signal because the two were travelling in a direction opposite to each other. The ratio between the pump and the signal also reduced due to pump power reduction as a result of attenuations within the fibre as it approached a stronger signal from the opposite end of the fibre. This in turn limited the pump to signal power transfer by a greater factor, which in turn increased the noise level within the fibre thus degrading the OSNR drastically. Co-pumping gave a better OSNR than counter pumping because co-pumping had a higher gain compared to counter pumping.

4.10 Noise Figure Analysis of SMF-Reach Fibre at different pumping configuration

Results in Fig 4.10 shows the experimental and simulation results of effective NF for co- and counter pumping schemes for 25 km fibre length.

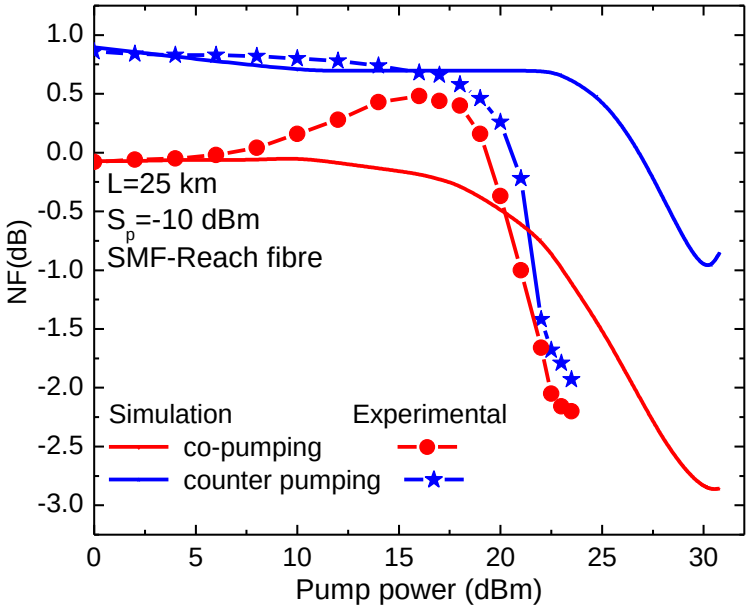

Fig 4-10: NF variations with pump power for co-pumping and counter pumping schemes, experimental and simulation results.

It is evident that the NF for co-pumping increased gradually with increase in pump power up to 17 dBm because this pump powers were low to induce SRS hence a continuous increase in pump power lead to more pump to signal relative intensity noise (RIN) transfer to the signal. RIN was more dominant in co- pumping than in counter pumping at pump powers of up to 17 dBm [62]. As the pump power increased beyond 17 dBm, the NF reduced with increase in pump power in the two pumping schemes. This is because the pump power over this region was now strong enough to boost the signal power thus accounting for the continuous decrease in the NF. Co-pumping gave a NF performance than counter pumping because for the case of co-pumping, both the pump power and the signal power were propagated in the same direction. This ensured that the pump was well

utilized by the signal thus more pump power was transferred to the signal hence higher amplification levels were achieved. Also the ratio between the pump power and the signal power was maintained almost at the same level throughout the transmission span. For the case of counter pumping, the signal was propagated in a direction counter to the pump. This limited the pump to signal power transfer thus leaving much of the pump power unutilized hence accounting for the higher NF attained in this pumping scheme.

Theoretical results were obtained through simulation of a 25 km fibre and having similar characteristics as the one used in the experiment. In this case, the NF reduced gently in the two pumping schemes for pump powers of up to 23 dBm because theoretical simulation assumed that the pump power over this range was not powerful enough to compensate for losses in the signal as it propagated through the fibre. Thus the signal power remained at low power over this region thus resulting to a higher NF over this power region. As pump power increased above 20 dBm the NF gradually reduced in both co- and counter pumping schemes.

Experimental measurement gave a higher NF compared to that attained obtained in the simulation. This was due to noise generation from passive components like connectors, isolators and WDM couplers which to some extent are polarization dependent loss devices. These components which are normally incorporated in any fibre optic system also add up losses to the signal during experimental measurements.

4.11 NF Analysis of co-pumping scheme for 25 km and 50 km SMF-Reach Fibres

Results in Fig 4.11 show how the effective NF varies with pump power for co- pumping at different pumping schemes.

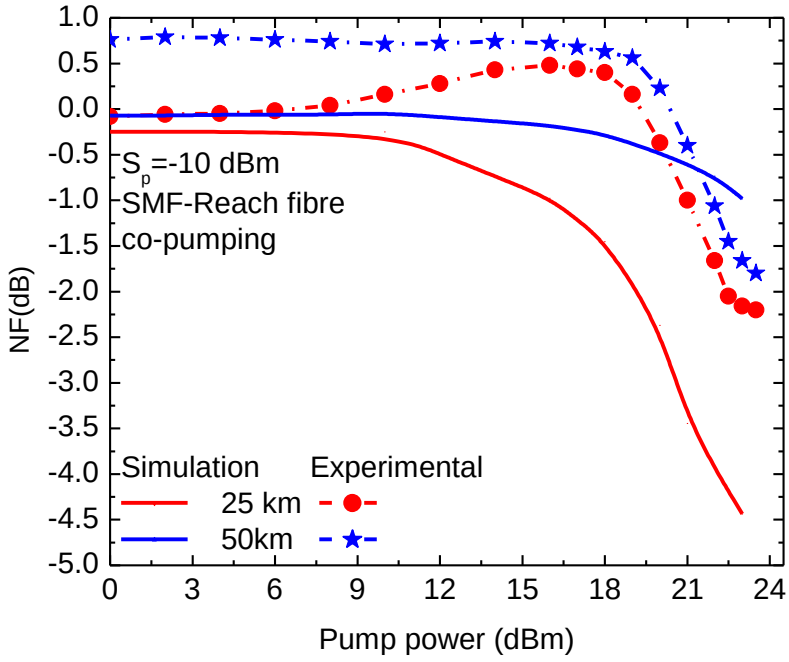

Fig 4-11: Effective Noise Figure (dB) as a function of pump power at different fibre lengths, experimental and simulation measurement.

It is clear that the NF increased slightly for pump powers of up to 17 dBm. This was due to RIN noise transfer to the signal which was dominant at this low pump powers. As the pump powers increased beyond 17 dBm, the NF decreased greatly in both fibre lengths because these pump powers were strong enough to amplify the signal thus compensating signal for losses within the transmission fibre.

A 50 km fibre gave a higher NF than a 25 km Fibre because as the fibre length increased, the contact time between the pump and the signal also increased thus more RIN noise transfer from the pump to the signal especially at lower pump powers. This increase in fibre length also leads to an increase in gain which in turn led to increased ASE noise generation in the process of attaining this higher gain.

Simulation results in Fig 4.11 were obtained with fibres of same lengths and characteristics. These results show a similar trend to the experimental results. . In this case, NF was lower because there were no losses at the connections as it was with experimental setup. Simulation results gave a lower NF compared to experimental results because passive components used in the experimental setup like connectors, isolators and WDM filters changed the SOP of the signal thus altering with its gain which in turn increased the experimental NF slightly. Under theoretical simulations, it was assumed that these passive components maintained the same SOP through the transmission span.

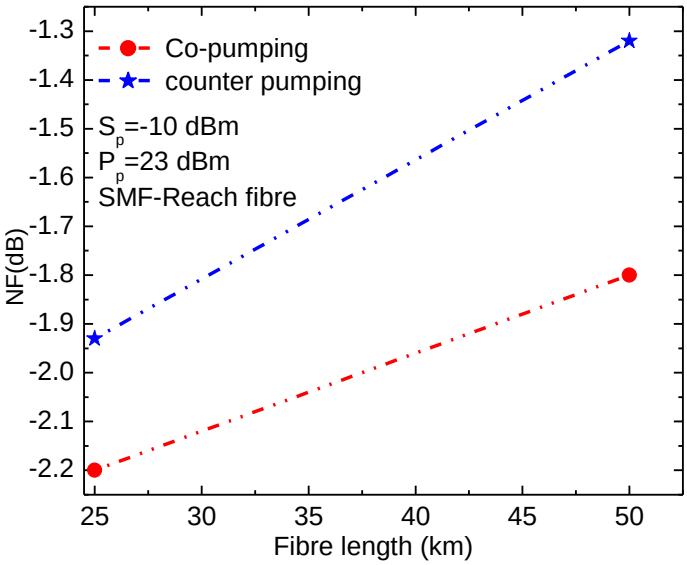

Fig 4-12:Effective Noise Figure (dB) verses fibre length (Km) at different pumping schemes.

Fig 4.12 shows the Noise Figure as a function of fibre length for co- and counter pumping schemes. From the results in Fig 4.12, an increase in fibre length led to an increase in NF because an increase in fibre length also led to an increase in the contact time between the pump and the signal thus more pump to signal noise transfer. Noise accumulation within the fibre also increases with increase in fibre length as a result of

attenuations. A higher gain was then attained which in turn led to an increase in ASE noise generation in the process of attaining this higher gain. This accounts for the increase in NF.

Counter pumping gave higher NF compared to that of co- pumping because in the case of counter pumping, the pump power was not well utilized by the signal because the two were travelling in a direction opposite to each other. This in turn limited the pump to signal power transfer by a greater factor. This alone limited the gain levels thus accounting for the higher NF recorded. Co-pumping gave a better NF performance than counter pumping because co-pumping had a higher gain compared to counter pumping.

CHAPTER FIVE

CONCLUSION AND RECOMMENDATIONS

5.1 Conclusion

Optical noise effects in optical fibres and optical communication components have been a subject of great interest and concern in the implementation of optical fibre technology. In this thesis, the effects of optical noise in distributed RFA designed using SMF-Reach and SMF-RS modern optical fibres were investigated. SRS which is a scattering phenomenon have been used to convert the fibre into an amplifying medium so that the signal strength can be restored and maintained within the fibre for long haul transmissions. The effect of Fibre lengths and pump powers, on-off gain, OSNR, NF and pump reflection have been studied at different pumping schemes.

The pump power was found to decrease exponentially with total length of the fibre in both pumping schemes. For pump power of up to 23 dBm and a fibre length of 25 km and an optimized signal power of -10 dBm, the Raman on-off gain was found to increase with fibre length and pump powers. The Co- pumping configuration provided a higher Raman on-off gain than counter pumping scheme. An on-off gain of 5.7 dB and 4.5 dB was achieved experimentally for co- and counter pumping schemes, respectively, for the 25 km SMF-Reach fibre. For a similar length of SMF-RS fibre, an on-off gain of 4.8 dB and 3.9 dB was achieved for co- and counter pumping schemes, respectively, for the 25 km fibre. For a 50 km fibre, an on-off gain of 6.6 dB and 5.1 dB was obtained for the two pump configurations respectively using SMF-Reach fibre. For a similar length of SMF-RS fibre, an on-off gain of 5.3 dB and 4.3 dB was achieved for co- and counter pumping

schemes, respectively. Pump reflection power was noticed to vary inversely with gain. An Optical Signal to Noise Ratio (OSNR) of 12.8 dB and 12.3 dB was achieved experimentally for co- and counter pumping schemes, respectively, for 25 km SMF-Reach. For 50 km fibre, an OSNR of 10.0 dB and 9.3 dB was recorded for the two pumping schemes respectively. OSNR was also observed to vary inversely with fibre length. The co-pumping configuration had a higher on-off gain and better OSNR performance than counter pumping scheme at similar fibre length and fibre type. Similarly, co- pumping scheme also had a better NF performance as opposed to counter pumping technique. SMF-RS fibre had a higher pump reflection power than SMF-Reach fibre of similar length and pumping technique.

5.2 Recommendations

This research work strongly advocates for the use of OFRA in long haul transmission of data due to its remarkable signal power recovery. A forward pumping configuration should be implemented especially in long haul signal transmission systems due to its low noise levels as opposed to backward. An SMF-Reach fibre should also be used in Raman amplification due to its higher gain and OSNR and low pump reflection power and NF. An extensive research on the methods of improving the Noise Figure should also be carried out especially on modern fibres which are currently used as amplifying mediums.

In the experimental work done, Raman pumps with maximum power supply of up to 23 dBm were used. Future work should be done using more powerful Raman pumps in signal amplification and its effect on OSNR, NF and noise performance analyzed at different pumping schemes. An extensive research should be carried out using bidirectional

pumping techniques and its performance on on-off gain, OSNR and NF also analyzed. Future work should be done using other modern fibre types and different signal sources.

LIST OF REFERENCES

[1] Keiser G., *Optical fibre communication*, 4th ed., New York, NY: McGraw-Hill, 2011.

[2] Senior J., *Optical fibre communications: Principals and practice*, 3rd ed., Prentice Hall, 2008.

[3] Becker P. C., Olsson N. A., and Simpson J. R., "Erbium-Doped Fiber Amplifiers Fundamentals and Technology," Academic Press, San Diego, CA, (1999).

[4] Thyagarajan K., and Ghatak A., "Some Important nonlinear effects in optical fibres Guided Wave Optical Components and Devices: Basics, Technology, and Applications," Bishnu P. Pal, Ac. Press, pp. 91-121, (2006).

[5] Eskildsen L., Hansen P. B., Grubb S.G., Stentz A. J., Strasser T.A., Judkins J., DeMarco J. J., Pedrazzani R., and DiGiovanni D. J., " Capacity upgrade of transmission systems by Raman amplification," Optical Amplifiers and Their Applications, Monterey, CA, Paper ThB4, (1996).

[6] Srivastava K., and Sun Y., "Advances in Erbium-Doped Fibre Amplifiers," Academic Press, pp. 174–212, (2002).

[7] Mori T., Masuda H., Shikano K., and Shimizu M., "Ultra-wide-band tellurite-based fibre Raman amplifier," Journal of Lightwave Technology, pp. 1300-1306, (2003).

[8] Monroy T., Kjær R., Öhman F., Yvind K., Jeppesen P., "Distributed fibre Raman amplification in long reach PON bidirectional access links," Optical Fibre Technology (Elsevier), vol. 14, pp. 41-44, (2008).

[9] Grubb S. G., Strasser T. A., Cheung W. Y., Reed W. A., Mizrahi V., Erdogan T., Lemaire P. J., Vengsarkar A. M., and DiGiovanni D. J., "High power 1.48 mm cascaded Raman laser in germanosilicate fibers," Optical Amplifiers and Their Applications, Davos, Switzerland, pp. 197, (1995).

[10] Seo H. S., Ghio Y. G., and Kim K. H., "Design of transmission optical fibre with a high Raman gain, large effective area, low nonlinearity and low double Rayleigh backscattering," IEEE photonic technol. lett., pp. 16, (2004).

[11] Perlin V. E., and Winful H. G., "On distributed Raman amplification for ultrabroad-band long-haul WDM systems," J. Lightwave Technol., vol. 20, pp. 409–416, (2002).

[12] Dakss M. L., and Melman P., "Amplified Spontaneous Raman Scattering and Gain Fibre Raman Amplifier," Journal of Lightwave, Tech. Vol. 6, (1985).

[13] Namiki S., and Emori Y., "Ultra broad-band Raman amplifiers pumped and gain-equalized by wavelength-division-multiplexed high-power laser diodes," *IEEE J. Select. Topics Quantum Electron.*, vol. 7, (2001).

[14] Raman C. V., "A new radiation," Indian J. Phys., Vol. 2, pp. 387, (1928).

[15] Woodbury E. J., and Nag W. K., "First demonstration of stimulated Raman scattering," Proc. IRE 50, pp. 2347, (1962).

[16] Ashcroft N. W., and Mermin N. D., *Solid State Physics*, Philadelphia, PA: Saunders College, 1976.

[17] Parakhan M. J., "Characteristic of Discrete Raman Amplifier at Different Pump Configuration," World Ac. Of Sci. Eng. & Techno., pp. 54, (2009).

[18] Singh S. P., Gangwar R., and Singh N., "Nonlinear scattering effects in optical fibres," Progress in Electromagnetics Research, PIER 74, pp. 379–405, (2007).

[19] Stolen R. H., Ippen E. P., and Tynes A. R., "Raman Oscillators in Glass Optical Waveguides," Applied Physics Lett., Vol. 20, pp. 62-64, (1992).

[20] Zhan X., and Magill P., "Polarization Dependent Gain due to Signal-Signal Raman Interaction; can Fibre PMD be too low?," in OFC, paper WE6, (2004).

[21] Stolen R. H., Gordon J. P., Tomlison W. J., and Haus H. A., "Raman Response Function of Silica- Core Fibre," J. Optical Soc. Amer. B, Vol. 6, pp. 1159-1166, (1989).

[22] Clifford H., and Agrawal G. P., *Raman Amplification in Fibre Optical Communication Systems*, Elsevier Ac. Press, USA, 2005.

[23] Dominic V., Mao E., Zhang V, Fidric B., Sanders S., and Mehuys D., "Distributed Raman amplification with co-propagating pump light," in Optical Amplifiers and Their Applications OSA Tech. Dig. Washington, DC, (2001).

[24] Lewis S. A., Chernikov S. V., and Taylor J. R., "Temperature-dependent gain and noise in fiber Raman amplifiers," Opt. Lett., vol. 24, no. 24, pp. 1823–1825, (1999).

[25] Agrawal G. P., *Fibre Optical Communications Systems*, 3rd Edition, John Willey& Sons, inc., 2002.

[26] Sun Y., Lima I., Lima A., Jiao H., Zweck J., Yan L., Menyuk C., and Carter G., "Effects of partially polarized noise in a receiver," in Proc. Optical Fiber Communications Conf., (2003).

[27] Stolen R. H., "Polarization Effects in Fibre Raman and Brillouin Lasers," IEEE Journal of Quantum Electronics, QE-15, pp.1157, (1979).

[28] Zhang W., Chen J., Peng J., Liu X., and Fan C., "An analytical method for determining comprehensive impact of Rayleigh backscattering on performance of systems with distributed Raman amplifiers," Lasers and Electro- Optics Society, 14th Annual Meeting of the IEEE, LEOS, No.1, pp. 350–351, (2001).

[29] Chang S. H., Kim S. K., Chu M. J., and Lee J. H., "Limitations in fibre Raman amplifiers imposed by Rayleigh scattering of signals," Electron. Lett., Vol. 38, No. 16, pp. 856–867, (2002).

[30] Wan P., and Conradi N., "Impact of double Rayleigh backscatter noise on digital and analog fibre systems," J. Lightwave Technol., Vol. 14, No. 3, pp 288–297, (1996).

[31] Hansen P. B., Eskildsen L., Stentz J., Strasser T. A., Judkins J., DeMarco J., Pedrazzani R., and DiGiovanni D. J., "Rayleigh scattering limitations in distributed Raman pre-amplifiers," Photonics Technology Letters, IEEE, Vol. 10, No. 1, pp. 159-161, (1998).

[32] Nissov M., Rottwitt K., Kidorf H. D., and Ma M. X., "Rayleigh crosstalk in long cascades of distributed unsaturated Raman amplifiers," Electronics Letters, Vol. 35, No.12, pp. 997-998, (1999).

[33] Chinn S. R., "Temporal observation and diagnostic use of double Rayleigh scattering in distributed Raman amplifiers," Photonics Technology Letters, IEEE, Vol.11, No.12, pp. 1632-1634, (1999).

[34] Matos C. J. S., Chestnut D. A., and Taylor J. R., "Continuous-wave-pumped Raman-assisted fibre optical parametric amplifier and wavelength converter in conventional dispersion-shifted fibre," Optics Letters, Vol. 26, No. 20, pp. 1583-1585, (2001).

[35] Kim C. H., Bromage J., and Jopson R. M., "Reflection-induced penalty in Raman amplified systems," Photonics Technology Letters, IEEE, Vol. 14, No. 4, pp. 573-575, (2002).

[36] Smith R. G., "Optical power handling capacity of low loss optical fibre as determined by stimulated Raman and brillouin scattering," Appl. Opt., Vol. 11, No. 11, pp. 2489–2494, (1972).

[37] Auyeung J., and Yariv A., "Spontaneous and stimulated Raman scattering in long low loss fibres," IEEE J. Quantum Electron., Vol. QE-14, pp. 347–352, (1978).

[38] Desurvire E., Digonnet M. J. F., and Shaw H. J., "Theory and implementation of a Raman active fibre delay line," J. Lightwave Technol., Vol. LT-4, pp. 426–443, (1986).

[39] Yariv A., *Optical Electronics in Modern Communications*, 5th ed. Oxford University Press, New York, Chap. 16, 1997.

[40] Fludger C. R. S., Handerek V., and Mears R. J., "Pump to signal RIN transfer in Raman fiber amplifiers," J. Lightwave Technol., vol. 19, pp. 1140–1148, (2001).

[41] Ohki Y., Hayamizu N., Shimizu H., Irino S., Yoshida J., Tsukiji N., and Namiki S., "Increase of relative intensity noise after fiber transmission in co-propagating Raman pump lasers," in Proc. Optical Amplifiers and Their Applications, (2002).

[42] Fludger C. R. S., Handerek V., and Mears R. J., "Fundamental noise limits in broadband Raman amplifiers," in Proc. Optical Fiber Communications Conf., (2001).

[43] Nakamura K., Yoshida M., Hidaka S. T., and Mitsuhashi Y., "Raman amplification of 1.50-μm laser diode light in a low fibre loss region," Journal of Lightwave Technology, Vol. 2, No. 4, pp. 379-381, (1984).

[44] Kuzin E., Mendoza-Vazquez S., Gutierrez-Gutierrez J., Ibarra-Escamilla B., Haus J., and Rojas-Laguna R., "Intra-pulse Raman frequency shift versus conventional Stokes generation of diode laser pulses in optical fibers," Optics Express, Vol. 13, No. 9, pp. 3388-3396, (2005).

[45] Aoki Y., "Fibre Raman amplifier properties for applications to long-distance optical communications," Optical and quantum electronics, Vol. 21, No. 1, pp. S89-S104, (1989).

[46] Gordon J. P., and Mollenauer L. F., "Phase noise in photonic communications systems using linear amplifiers," Optics letters, Vol. 15, No. 23, pp. 1351-1353, (1990).

[47] Nissov M., Davidson C. R., Rottwitt K., Menges R., Corbett P. C., Innis D., and Bergano N. S., "100 Gb/s (10× 10 Gb/s) WDM transmission over 7200 km using distributed Raman amplification," In Integrated Optics and Optical Fibre Communications, 11th International Conference on, and 23rd European Conference on Optical Communications, Conf. Publ. No.: 448, Vol. 5, pp. 9-12, IET, (1997).

[48] Nissov M., Rottwitt K., Kidorf H. D., and Ma M. X., "Rayleigh crosstalk in long cascades of distributed unsaturated Raman amplifiers," Electronics Letters, Vol. 35, No. 12, pp. 997-998, (1999).

[49] Van Deventer M. O., "Polarization properties of Rayleigh backscattering in single-mode fibres," Journal of Lightwave Technol., Vol.11, pp. 1895, (1999).

[50] Islam M., *Raman Amplifiers for Telecommunications 2: Sub-systems and Systems,* Springer-Verlag, New York, pp. 491, (2004).

[51] Derickson D., *Fibre Optic Test and Measurement*, Prentice Hall, Upper Saddle River, NJ, (1998).

[52] Dimitropoulos D., Solli R. D., Claps R., Boyraz O., and Jalali B., "Noise Figure of Silicon Raman Amplifiers," Journal of Lightwave technology, Vol. 26, No. 7, (2008).

[53] Tricker R., *Optoelectronics and fiber optic technology,* Newnes, (Elsevier Ltd), 1st ed., 2002.

[54] Spirit D. M., Ellis A. D., and Barnsley P. E., "Optical time division multiplexing: systems and networks," *Communications Magazine, IEEE*, vol. 32, no.12, pp. 56-62,(1994).

[55] Bononi A., and Vannucci A., "Degree of polarization degradation due to cross-phase modulation and its impact on polarization-Mode Dispersion compensators," J. Lightwave Technol., vol. 21, pp.1903-1913, (2003).

[56] Agrawal G. P., *Nonlinear Fiber Optics*, chapter six, 4th ed. San Diego, CA: Academic, 2007.

[57] Jeunhome L. B., *Single-Mode Fiber Optics Principles and Applications,* Dekker, New York, pp.100, 1990.

[58] Shen Y. R., *The Principles of Nonlinear Optics,* Wiley, New York, Chap. 10, 1984.

[59] Virtual Photonics, Inc. (VPI), version 9.0 http://www.virtualphotonics.com.

[60] Mathur A., Ziari M., Hagberg M., "Trends in Optics and Photonics," OSA, Series OAA 99, Vol. 30 pp. 187, (1999).

[61] OFS' TrueWave®, "Optimized for lowest total systems cost of EDFA-amplified networks in metro, regional, and long haul applications," data sheet, Doc ID: fibre-124, Publish Date: 0313.

[62] Bromage J., "Raman Amplification for Fiber Communications Systems," journal of lightwave technology, vol. 22, no. 1, (2004).

APPENDICES

APPENDIX I

Journal and Conference Publications

[1] **G. M. Isoe**, K. M. Muguro, and D. W. Waswa, *"Noise Figure Analysis of Distributed Fibre Raman Amplifier*," international journal of scientific & technology research vol. 2, issue 11, ISSN: 2277-8616, pp. 375-378, November 2013.

[2] **G. M. Isoe**, K. M. Muguro, D. W. Waswa, E. K. Rotich Kipnoo, T. B. Gibbon, and A.W. R. Leitch, "*Effects of Double Rayleigh Scattering in Fibre Raman Amplifier at Different Pump Configurations*," Proceedings of Southern African Telecommunication Networks and Application Conference (SATNAC) 2013, ISBN: 978-0-620-57883-7, pp. 49-53, September 2013.

[3] **G. M. Isoe**, K. M. Muguro, D. W. Waswa, D. Osiemo, E. Kirui, H. Cherutoi, D. K. Boiyo, and E. K. Rotich Kipnoo, "*Forward Raman Amplification Characterization in Optical Networks,*'' Proceedings of 2014 international conference on Sustainable Research and innovation (SRI), Vol. 5, ISSN: 2079-6226, pp. 251-253, May 2014.

[4] D. M. Osiemo, D. W. Waswa, K. M. Muguro, **G. M. Isoe**, E. Kirui, and H. Cherutoi, "*Brillouin Threshold Measurement in Optical Fibres,*" Proceedings of 2014 international conference on Sustainable Research and innovation (SRI), Vol. 5, ISSN: 2079-6226, pp. 243-246, May 2014.

[5] **G. M. Isoe**, K. M. Muguro, D. W. Waswa, E. K. Rotich Kipnoo , T. B. Gibbon, and A.W. R. Leitch, "*Performance Comparison of SMF-Reach and SMF-RS*

Optical Fibres for Raman Amplification,'' Poster presentation at the 59th South African Institute of Physics (SAIP) Conference, the University of Johannesburg, South Africa, 7th -11th July 2014.

[6] **G. M. Isoe**, K. M. Muguro, D. W. Waswa, E. K. Rotich Kipnoo, T. B. Gibbon and A.W. R. Leitch, "*Analysis of Optical Signal to Noise Ratio in Modern Transmission Fibres during Raman Amplification,*" Southern African Telecommunication Networks and Application Conference (SATNAC) at The Boardwalk, Port Elizabeth, Eastern Cape, South Africa, 31st Aug. – 3rd Sept., 2014. —– Accepted for oral presentation.

Research Visit

Optical Fibre Technologies Research and Discussions, Nelson Mandela Metropolitan University, Port Elizabeth, South Africa, 8th March- 29th may 2014.

APPENDIX II

Components used in experimental work

Optical power meter

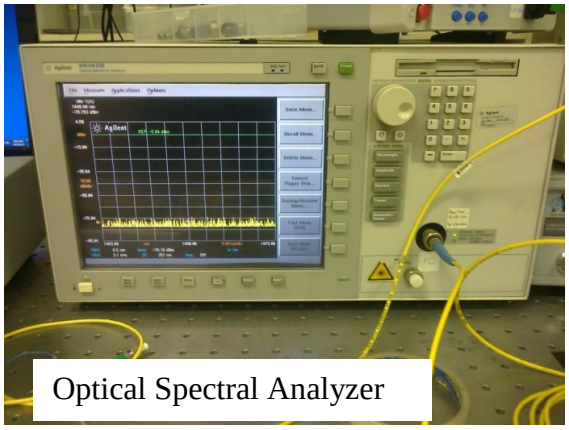

Optical Spectral Analyzer

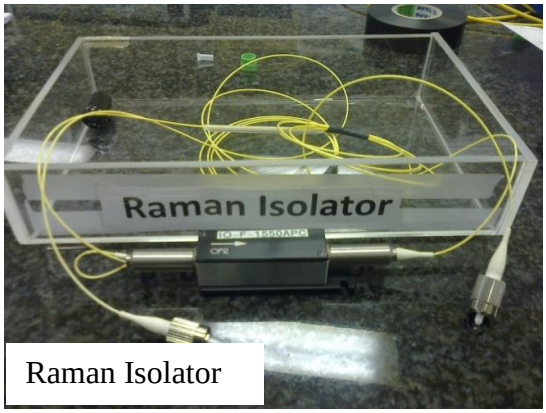

Raman Isolator

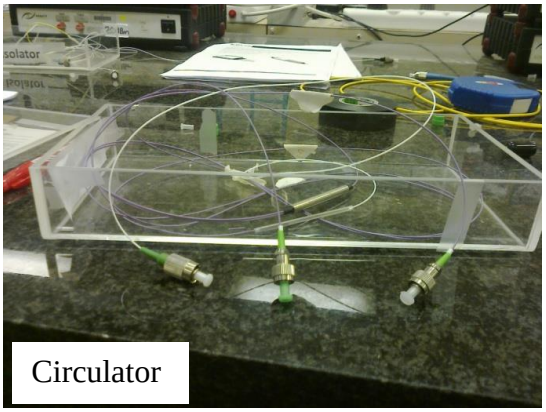

Circulator

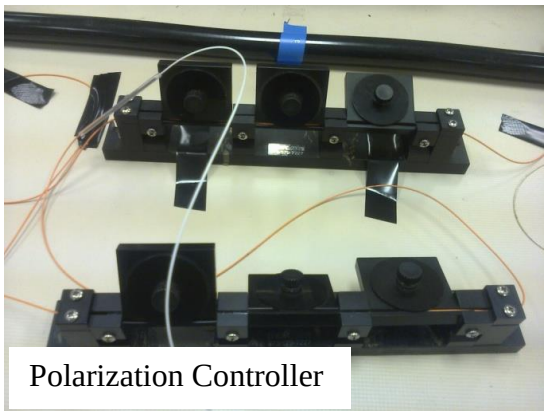

Polarization Controller

Tunable Laser Source

(Optical Fibre Technologies Research and Discussions, Nelson Mandela Metropolitan University: (Source: Author, 2014)

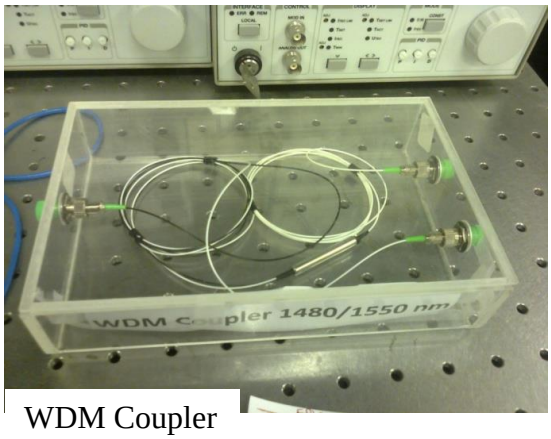

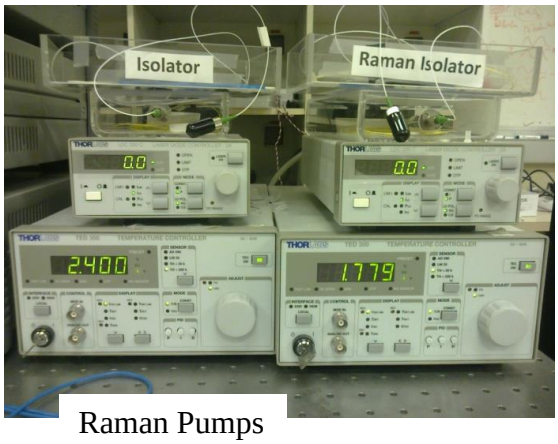

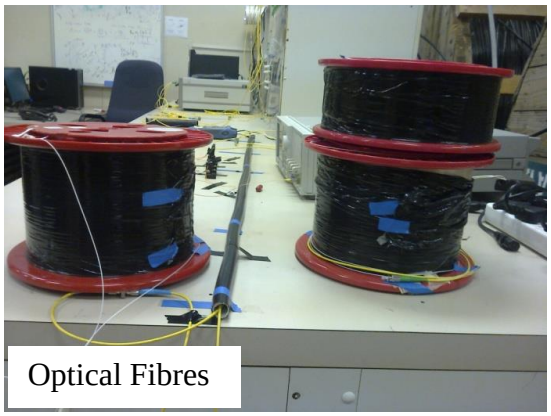

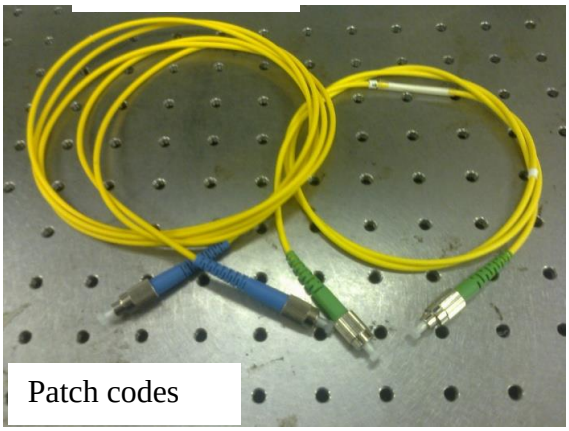

(Optical Fibre Technologies Research and Discussions, Nelson Mandela Metropolitan University: (Source: Author, 2014)